

CHAPTER 3 UNBOUND MATERIALS TESTING FOR CONSTRUCTION QUALITY DETERMINATION

The initial testing under Part A of the experimental plan was to confirm that the NDT technologies can identify differences in construction quality of unbound pavement layers. The specific hypothesis used for this part of the experiment was that the NDT technology and device can detect changes in the physical condition of the materials. Table 14 summarizes the differences between the unbound materials placed along each project. During nondestructive testing, none of the NDT operators were advised of those differences listed in table 14.

This chapter of the Phase 2 – Part A interim report presents the NDT responses measured on the unbound materials at each project discussed in Chapter 2. It also provides a brief evaluation of the materials based on those measured responses and compares the responses measured by different NDT devices on the same material.

Table 14. Description of the Different Physical Conditions of the Unbound Materials and Soils Placed Along Each Project

Project Identification	Unbound Sections	Description of Differences Along Project
SH-21 Subgrade, High Plasticity Clay; Caldwell, Texas	Area 2, No IC Rolling	No planned difference between the points tested.
	Area 1, With IC Rolling	With IC rolling, the average density should increase; lane C received more roller passes.
I-85 Embankment, Low Plasticity Clay; Auburn, Alabama	Lane A of Sections 1 & 2 (refer to figure 17)	Prior to IC rolling, Lane A (which is further from I-85) had thicker lifts & a lower density.
	All sections tested	After IC rolling, the average density should increase & the variability of density measurements should decrease.
TH-23 Embankment, Silt-Sand-Gravel Mix; Spicer, Minnesota	South Section – Lane C (refer to figure 3.a)	Construction equipment had disturbed this area. In addition, QA records indicate that this area has a lower density.
	North Section – Lane A (refer to figure 3.a)	The area with the higher density and lower moisture content – a stronger area.
SH-130, Improved Embankment, Granular; Georgetown, Texas	All sections tested	No planned differences between the areas tested.
TH-23, Crushed Aggregate Base; Spicer, Minnesota	Section 2 (middle section) – Lane C (refer to figure 3.b)	Curb and gutter section; lane C was wetter than the other two lanes because of trapped water along the curb from previous rains. The water extended into the underlying layers.
	Section 1 (south section) – Lane A (refer to figure 3.b)	Area with a higher density and lower moisture content; a stronger area.
US-280, Crushed Stone Base; Opelika, Alabama	Section 4	Records indicate that this area was placed with higher moisture contents and is less dense. It is also in an area where water (from previous rains) can accumulate over time.

3.1 NDT Technologies

3.1.1 Dynamic Cone Penetrometer Testing

The manual DCP was used to estimate the in situ shear strength of the unbound materials in accordance with ASTM D6951. However, the sequence of drops and penetration readings were modified based on the layer thickness and material being evaluated at each project site. Figure 26 shows the DCP being used to measure the in situ strength of the embankment soil in Minnesota.



Figure 26 Dynamic Cone Penetrometer testing to estimate the in situ shear strength of unbound materials (courtesy MnRoads).

For each point, the test was begun by using one seating drop from full height. The penetration was recorded for the seating drop. The penetration was then recorded after each drop or five successive drops throughout the layer thickness, depending on its strength. One DCP test was performed at each test point. At a few test locations, however, refusal of the DCP occurred when large aggregate were encountered when testing the TH-23 embankment material. When refusal occurred, the DCP was moved slightly and the test repeated.

The penetration rate has been correlated to resilient modulus, as presented in the Phase 1 interim report (Von Quintus, et al., 2004). Equation 1 was used to calculate the resilient modulus for each test point. Table 15 lists the average resilient modulus values for each area tested. The DCP test or penetration of the device was continued into the supporting layer. All incremental penetration rates are provided in the appendix. However, only the average

penetration rate through the test material was used to calculate the elastic modulus at each test point.

$$E_R = 17.6 \left(\frac{292}{(DPI)^{1.12}} \right)^{0.64} \quad (1)$$

Where:

- E_R = Resilient modulus, MPa.
 DPI = Penetration rate or index, mm/blow.

Table 15 – Summary of Resilient Modulus Calculated from the Dynamic Cone Penetrometer Test Results Using Equation 1, ksi

Project ID		A	B	C	D
I-85 Low Plasticity Clay; Section 1; Before IC Rolling	Mean	5.41	6.71	6.04	5.47
	COV, %	13.7	48.4	29.4	24.3
I-85 Low Plasticity Clay; Section 2; Before IC Rolling	Mean	4.98	5.32	5.44	4.73
	COV, %	11.9	25.2	22.7	25.2
I-85 Low Plasticity Clay; Section 1; After IC Rolling	Mean	6.66	7.74	7.10	6.23
	COV, %	19.5	38.0	24.7	26.6
I-85 Low Plasticity Clay; Section 2; After IC Rolling	Mean	6.07	6.20	6.54	6.01
	COV	18.5	15.3	12.5	26.5
SH-21, High Plasticity Clay; Area 2, No IC Rolling	Mean	---	---	---	11.9
	COV, %	---	---	---	16.6
SH-21, High Plasticity Clay; Area 1, With IC Rolling	Mean	9.1	8.3	9.9	---
	COV, %	40.2	16.8	19.1	---
TH-23 Embankment, Silt-Sand- Gravel Mix; South Section	Mean	14.77	15.55	11.47	---
	COV, %	4.8	14.8	22.3	---
TH-23 Embankment, Silt-Sand Gravel Mix; North Section	Mean	18.52	20.22	17.80	---
	COV, %	21.5	26.2	28.3	---
SH-130 Granular, Improved Embankment; Section 1	Mean	20.50	18.65	24.18	---
	COV, %	14.0	25.0	24.0	---
SH-130 Granular, Improved Embankment; Section 2	Mean	21.31	20.32	18.85	---
	COV, %	43.4	36.8	10.4	---
SH-130 Granular, Improved Embankment; Section 3	Mean	22.99	23.87	19.18	---
	COV, %	37.5	58.9	40.6	---
TH-23 Crushed Aggregate; Middle Section	Mean	42.25	33.07	18.55	---
	COV, %	46.6	38.3	20.0	---
TH-23 Crushed Aggregate; South Section	Mean	48.23	44.66	24.11	---
	COV, %	50.5	20.6	16.6	---
US-280, Crushed Stone; Section 1	Mean		53.79		---
	COV, %		23.8		---
US-280, Crushed Stone; Section 2	Mean		45.90		---
	COV, %		21.8		---
US-280, Crushed Stone; Section 3	Mean		51.19		---
	COV, %		8.9		---
US-280, Crushed Stone; Section 4	Mean		34.31		---
	COV, %		11.9		---

Note: The shaded cells designate those areas with anomalies (refer to table 14); black cells denote weaker areas, while the gray cells denote stronger areas for a specific project.

Figure 27 compares the standard deviation to the mean elastic modulus calculated from the DCP penetration rate for both fine and coarse-grained materials. As shown, the standard deviation increases with material strength or increasing elastic modulus. In addition, the coarse-grained materials were found to be consistently stronger than the fine-grained soils.

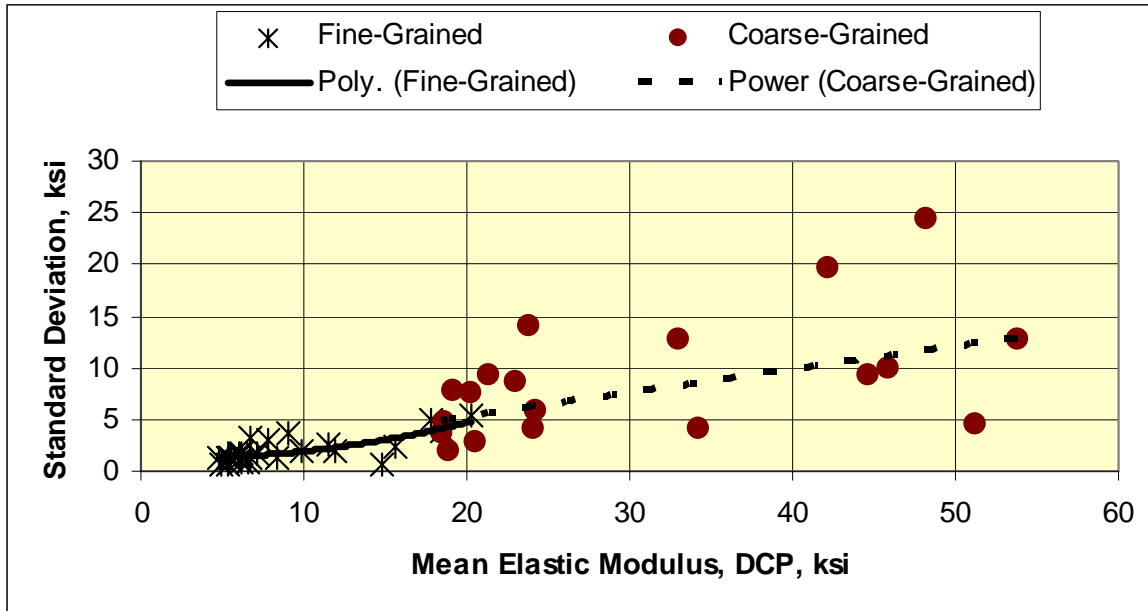


Figure 27 Relationship between the standard deviation and mean of the elastic modulus values of unbound materials calculated from the DCP penetration rate.

The cells in table 15 that correspond to those conditions listed in table 14 have been shaded. The following bullets summarize the results of the DCP tests in accordance with those conditions listed in table 14.

- I-85 Low Plasticity Soil Embankment – The DCP found both outside lanes (lanes A and D) to be weaker than the two inside lanes, both before and after IC rolling. The DCP results also indicate a consistent increase in the embankment’s strength after IC rolling, but not a reduction in variability of strength.
- SH-21 High Plasticity Clay Soil – The DCP found area 1, with IC rolling and testing, to be weaker than area 2. This observation is inconsistent with construction records. However, area 2 was found to have some gravel mixed in with the high plasticity clay near the surface (top 6 to 8 inches) during the sampling process. This could explain the higher strengths in area 2.
- TH-23 Gravelly, Silty Clay (Silt-Sand Gravel Mix) Embankment – The DCP correctly found lane C of the south section to be the weaker of the areas tested, and found the entire north section to be significantly stronger than the south section. Lane A was not stronger than the other two lanes tested in the north section, which is inconsistent with construction records.

- SH-130 Improved Granular Embankment – The DCP found no significant difference between the areas tested, which was planned.
- TH-23 Crushed Aggregate Base – The DCP found lane C in the middle section to be the weaker and lane A in the south section to be stronger. The paving schedule prevented the north section from being tested with the DCP.
- US-280 Crushed Stone Base – The DCP found area 4 to be softer of the four areas tested. However, its strength is still high and consistent with adequately compacted crushed stone.

3.1.2 Deflection Testing

Two types of deflection measuring equipment were used on some of the projects; the trailer mounted falling weight deflectometer (FWD) and the portable or lightweight deflectometer (LWD).

Falling Weight Deflectometer

Deflection basins were measured with the FWD in accordance with the test protocol being used in the Long Term Pavement Performance (LTPP) program. The procedure was to use two seating drops, followed by two drops at each drop height. Three drop heights were used at each test point. The deflection basins were recorded for each drop, including the seating drops. After the first set of tests, the FWD was moved forward (where the loading plate would be in contact with a different area) and the test sequence repeated. This sequence of drops and replicate testing was used at each test point. Figure 28 shows the FWD in operation. The larger diameter loading plate was used for all unbound materials testing, and the deflections were measured at seven sensors at the spacing recommended for use in LTPP.



Figure 28 Falling Weight Deflectometer



The deflection basins were used to forward calculate the elastic modulus of the layer being evaluated using the procedure developed by Stubstad, et al (Stubstad, et al., 2003). The calculated elastic modulus values are summarized in table 16 for the US-280 project. Elastic moduli were also back-calculated using other traditional methods and more sophisticated pattern recognition methods. The forward calculation method resulted in the least variation of elastic moduli within a specific area.

Project ID	Area	A	B	C	D
US-280; Crushed Stone; Section 1	1	18.1	15.7	15.7	---
	2	8.10	6.3	7.2	---
	3	16.7	17.9	20.2	---
	4	27.5	26.8	25.9	---
	5	32.3	35.1	38.3	---
	Mean	20.794			---
	Std. Dev.	9.979			---
	COV, %	48.0			---
US-280; Crushed Stone; Section 2	1	16.6	13.8	---	---
	2	11.9	8.6	9.2	---
	3	15.5	18.2	14.9	---
	4	26.4	32.1	30.0	---
	5	---	31.4	28.7	---
	Mean	19.798			---
	Std. Dev.	8.686			---
	COV, %	43.9			---
US-280; Crushed Stone; Section 3	1	32.3	31.7	26.9	---
	2	14.2	11.7	10.6	---
	3	7.8	8.2	9.2	---
	4	22.3	18.5	20.3	---
	5	20.3	18.7	19.6	---
	Mean	18.166			---
	Std. Dev.	7.969			---
	COV, %	43.9			---
US-280; Crushed Stone; Section 4	1	5.5	5.0	5.4	---
	2	5.7	5.4	5.7	---
	3	7.3	7.2	7.5	---
	4	7.5	6.6	7.7	---
	5	6.2	6.8	5.7	---
	Mean	6.352			---
	Std. Dev.	0.9196			---
	COV, %	14.5			---

Note: The shaded cells designate those areas with anomalies (refer to table 14); black cells denote weaker areas.

Portable or Lightweight Deflectometer

Deflections were also measured with different LWD devices in accordance with the manufacturer's recommendations. One to three LWD devices were used on the projects. These devices are defined as the Loadman, Dynatest Prima 100, and Carl Bro. The Loadman and Dynatest Prima 100 were used to measure the deflection at the center of the loading plate, while the Carl Bro device was used to measure the deflections under the loading plate and at two additional sensors spaced at 8 and 12 inches from the loading plate. Figure 29 shows the LWDs that were used on selected projects.

A seating drop was used to begin the test for each device. The seating load and deflection were recorded. The seating drop was followed by five successive drops. Elastic modulus values were calculated from the measured loads and deflections for each drop, in accordance with the procedures recommended by the individual manufacturers. The average elastic modulus values, excluding the seating drop, are provided in table 17 for the Carl Bro device. Table 18 lists the average elastic modulus values calculated from the loads and deflections measured with the other LWD devices (Dynatest Prima 100 and Loadman).

Comparison of Test Results from Deflection Based Devices

Figure 30 compares the average elastic modulus calculated from the loads and deflections measured with various deflection measuring devices. As shown, the Carl Bro device consistently measured higher elastic modulus values than the Dynatest Prima 100 and FWD. The elastic modulus values from the Loadman are more diverse for the weaker layers and much higher for the stronger layers (figure 30.a).

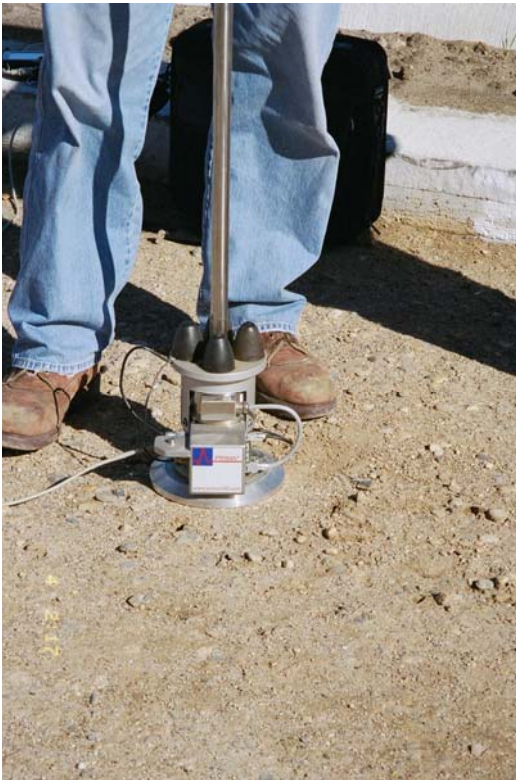
Figure 31 presents a cumulative frequency diagram of the standard deviation or repeatability of the deflection based methods. The standard deviations in figure 31 represent the variability between the five successive drops at the same test point. The repeatability of the LWD devices (excluding the Loadman device) is considered good, with a mean standard deviation less than 0.5 ksi.

Figure 32 compares the standard deviation of the measurements made within an area to the mean elastic modulus calculated for that area. As shown, the standard deviation continues to increase with increasing elastic modulus. Similar to the DCP, the LWD measured consistently higher elastic modulus values for coarse-grained materials than for fine-grained materials.

Figure 33 includes a comparison of the coefficient of variation in elastic modulus values determined with each of the deflection measuring devices to normalize differences caused by changes in material strength. The Carl Bro and Dynatest Prima 100 devices measured similar variability, while the Loadman device and FWD consistently measured higher variability. Thus, test results from the Carl Bro and Dynatest devices were used in comparison to the other NDT technologies.



(a) Loadman LWD used on selected projects.



(b) Loading plate for the LWD.



(c) Prima 100 LWD.

Figure 29 Lightweight deflectometers used for testing unbound materials and soils.

Table 17 – Summary of the Calculated Elastic Modulus from the CarlBro LWD Test Results, ksi

Project ID	Area	A	B	C	D
I-85 Low Plasticity Clay; Section 1; Before IC Rolling	Mean	---	---	---	---
	COV, %	---	---	---	---
I-85 Low Plasticity Clay; Section 2; Before IC Rolling	Mean	---	---	---	---
	COV, %	---	---	---	---
I-85 Low Plasticity Clay; Section 1; After IC Rolling	Mean	9.767	8.989	13.06	8.145
	COV, %	20.5	31.6	6.5	84.0
I-85 Low Plasticity Clay; Section 2; After IC Rolling	Mean	11.78			
	COV, %	47.1			
SH-21 High Plasticity Clay, Area 2; No IC Rolling	Mean	---	---	---	---
	COV, %	---	---	---	---
SH-21 High Plasticity Clay, Area 1; With IC Rolling	Mean	8.7	7.3	12.9	---
	COV, %	27.9	36.3	45.8	---
TH-23 Embankment, Silt-Sand- Gravel Mix; South Section	Mean	6.082	5.264	5.552	---
	COV, %	14.0	27.6	14.9	---
TH-23 Embankment, Silt-Sand- Gravel Mix; North Section	Mean	4.685	4.618	4.800	---
	COV, %	13.9	23.6	27.9	---
SH-130 Granular, Improved Embankment, Section 1	Mean	27.8	23.6	21.7	---
	COV, %	51.2	60.3	22.4	---
SH-130 Granular, Improved Embankment, Section 2	Mean	23.6	29.7	21.3	---
	COV, %	42.7	26.2	28.2	---
SH-130 Granular, Improved Embankment, Section 3	Mean	21.4	30.2	20.7	---
	COV, %	65.4	80.5	19.3	---
TH-23; Crushed Aggregate, Middle Section	Mean	15.45	12.80	7.95	---
	COV, %	53.6	42.8	9.0	---
TH-23 Crushed Aggregate, South Section	Mean	17.66	21.10	8.67	---
	COV, %	61.1	42.0	22.5	---
US-280 Crushed Stone; Section 1	Mean	51.23			---
	COV, %	56.1			---
US-280 Crushed Stone; Section 2	Mean	37.82			---
	COV, %	44.0			---
US-280 Crushed Stone; Section 3	Mean	50.334			---
	COV, %	42.2			---
US-280 Crushed Stone; Section 4	Mean	18.53			---
	COV, %	16.8			---

Note: The shaded cells designate those areas with anomalies (refer to table 14); black cells denote weaker areas, while the gray cells denote stronger areas within a specific project.

Table 18 – Summary of the Calculated Elastic Modulus from the Other LWD Test Results, ksi

Project ID	Area	Loadman LWD Device			Dynatest Prima 100		
		A	B	C	A	B	C
TH-23 Embankment; South Section	Mean	3.085	3.029	1.036	---	---	---
	COV, %	19.9	64.7	51.6	---	---	---
TH-23 Embankment; North Section	Mean	5.200	4.488	3.000	---	---	---
	COV, %	47.1	44.2	81.8	---	---	---
TH-23 Crushed Aggregate; Middle Section	Mean	25.922	44.704	16.026	---	---	---
	COV, %	46.0	74.4	31.5	---	---	---
TH-23 Crushed Aggregate; South Section	Mean	35.22	36.14	20.90	---	---	---
	COV, %	77.3	56.6	18.2	---	---	---
US-280 Crushed Stone; Section 1	Mean	---	---	---	32.87		
	COV, %	---	---	---	41.0		
US-280 Crushed Stone; Section 2	Mean	---	---	---	14.20		
	COV, %	---	---	---	37.2		
US-280 Crushed Stone; Section 3	Mean	---	---	---	26.21		
	COV, %	---	---	---	21.5		
US-280 Crushed Stone; Section 4	Mean	---	---	---	9.64		
	COV, %	---	---	---	20.3		

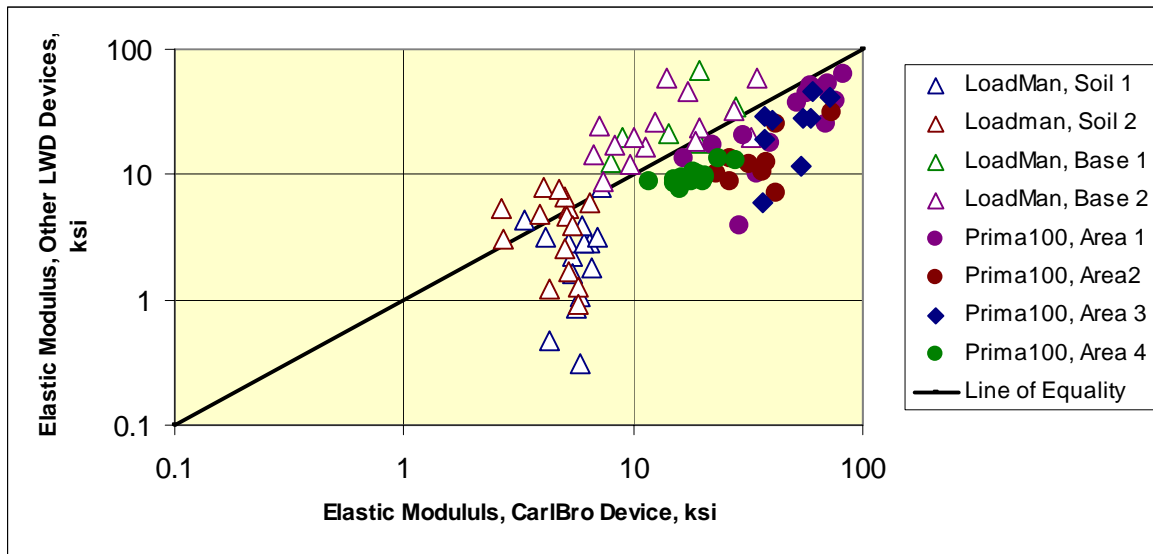
Note: The shaded cells designate those areas with anomalies (refer to table 14); black cells denote weaker areas, while the gray cells denote stronger areas tested with a specific project.

The cells in tables 16, 17, and 18 that correspond to those conditions listed in table 14 have been shaded. The following bullets summarize the results of the deflection-based methods in accordance with those conditions listed in table 14.

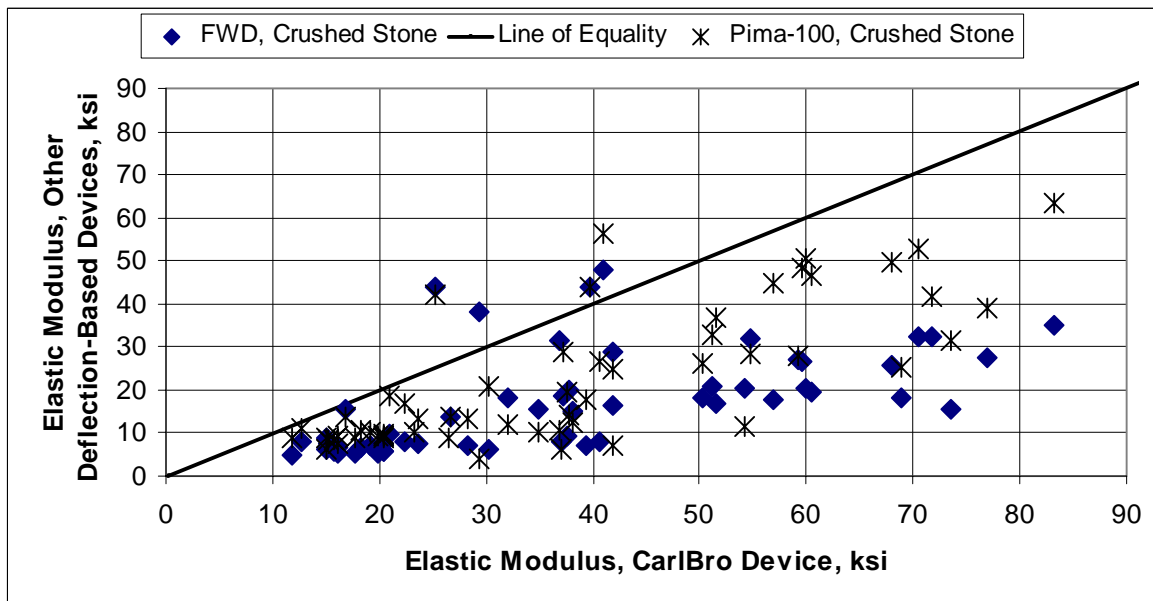
- I-85 Low Plasticity Soil Embankment – The deflection-based methods were not used to test the embankment prior to IC rolling. No significant difference in stiffness was found between the areas tested after IC rolling, as planned.
- SH-21 High Plasticity Clay – The deflection-based methods found lane C of area 1 to be stronger than lanes A and B, which is inconsistent with construction records.
- TH-23 Gravelly, Silty Clay Embankment – The deflection-based tests found no significant difference in stiffness between the areas tested in the south section, and found the north section to be weaker than the south section, with the exception of the Loadman device (refer to table 18). This finding is inconsistent with QA records and other tests. It is expected that the calculated modulus values are being influenced by the underlying foundation. The Loadman device resulted in low modulus values for the TH-23 embankment that are extremely variable. This result is questionable based on visual observations of construction traffic that was using this area.
- SH-130 Improved Granular Soil – The deflection-based methods found no consistent difference between the three areas tested, which was planned.
- TH-23 Crushed Aggregate Base – The deflection-based methods found lane C to be the weakest of all areas tested; similar to the results from the DCP. The paving schedule prevented the north section from being tested with the deflection-based

devices. The deflection-based methods also found the south section to be stronger than the middle section.

- US-280 Crushed Stone Base – The deflection-based methods found area 4 to be the weakest of the four areas tested, similar to the DCP results. However, the modulus values calculated from deflections for area 4 are inconsistent with a good quality crushed stone. It is expected that the calculated modulus in this area are being influenced (lowered) by the underlying layers.



(a) Other LWD devices, as compared to the CarlBro LWD device.



(b) FWD and Prima 100 devices, as compared to the CarlBro LWD device.

Figure 30 Comparison of the average elastic modulus calculated from deflections and loads measured with various LWD devices.

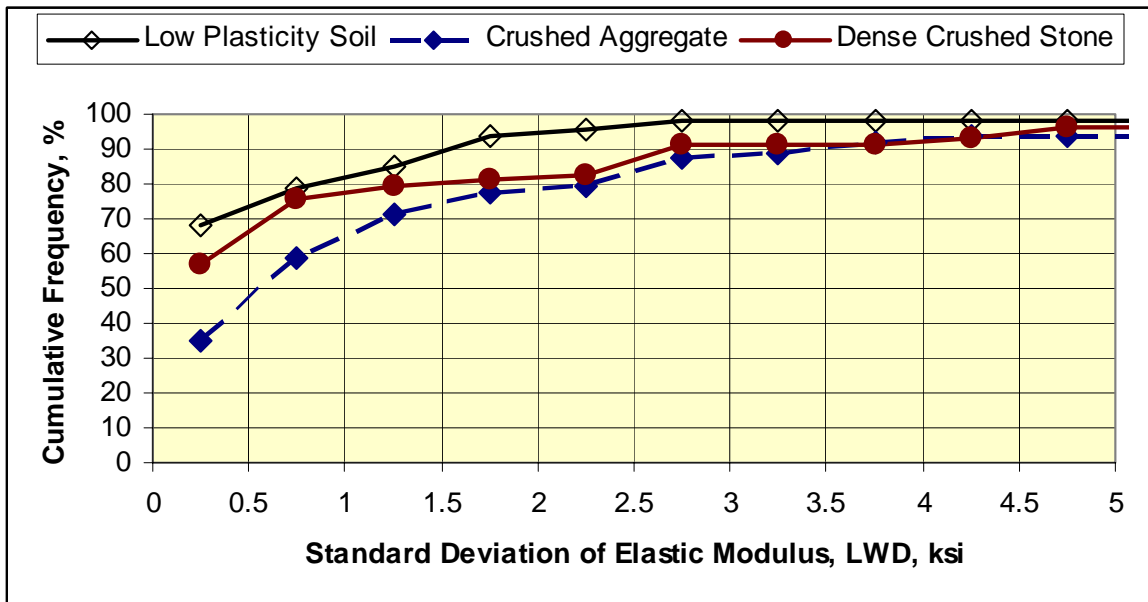


Figure 31 Cumulative frequency of the standard deviation from the deflection-based test methods.

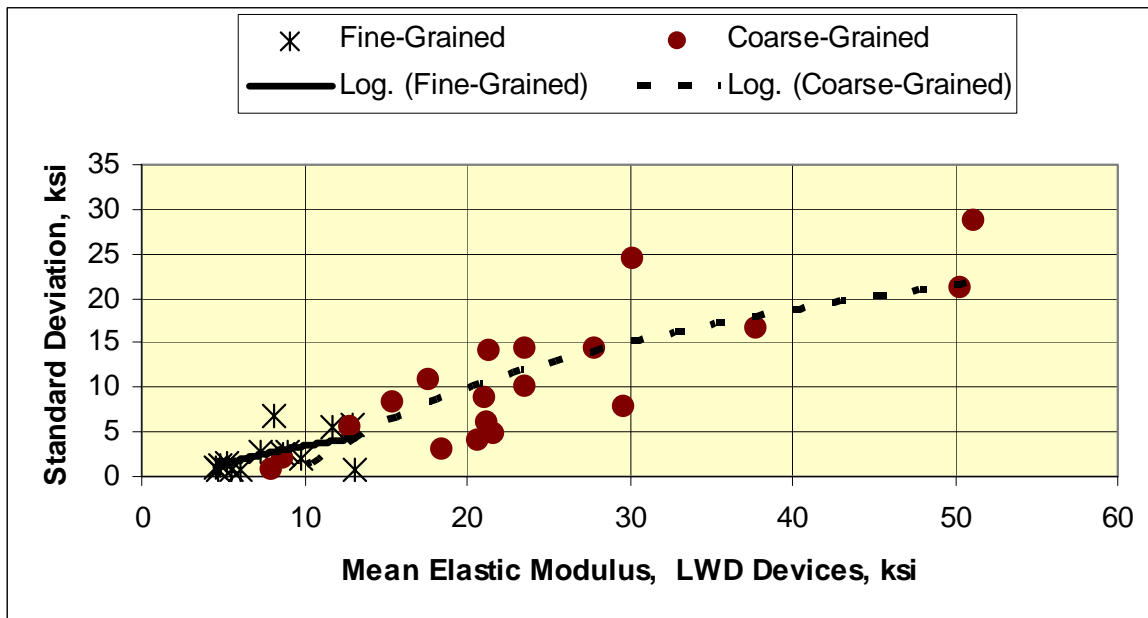


Figure 32 Relationship between the standard deviation and mean of the elastic modulus values of unbound materials calculated from the deflections.

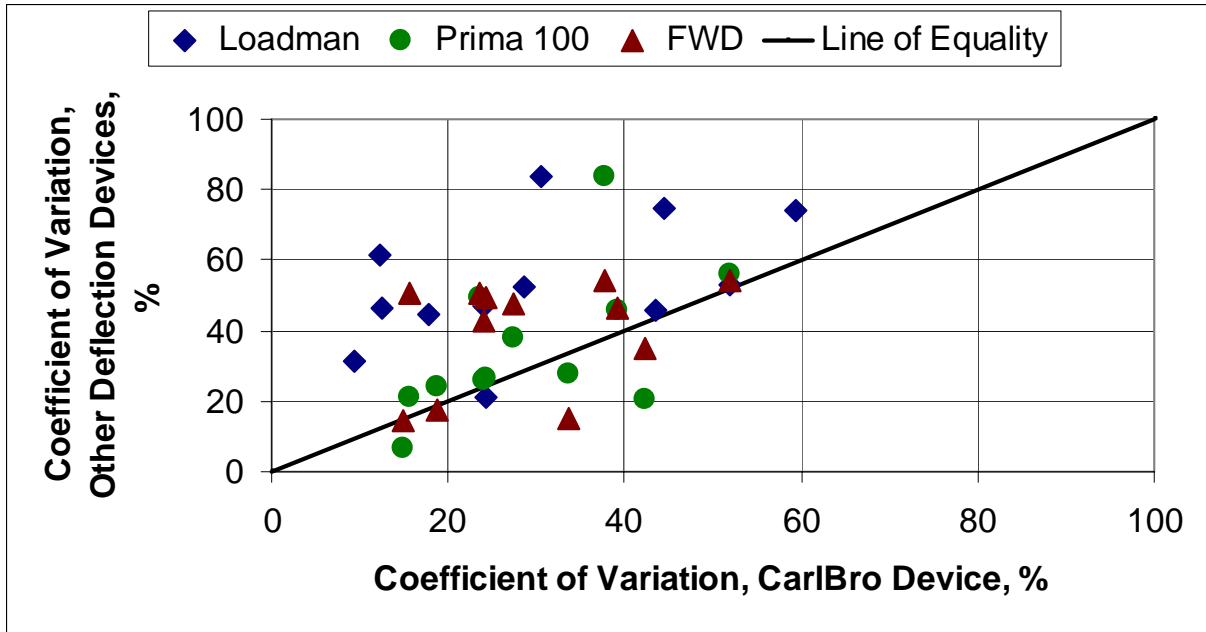


Figure 33 Comparison of the coefficient of variations for calculated elastic modulus from various deflection measuring devices.

3.1.3 Seismic Testing

Two devices were used to measure the elastic modulus of the unbound materials, which are discussed under this technology. These two devices are defined as the DSPA and the GeoGauge. Although these two devices are included under the same NDT technology grouping, they are significantly different.

DSPA

The DSPA was used to measure the seismic modulus of the unbound materials in accordance with the procedure developed by Dr. Nazarian for the Texas DOT (Nazarian, et al., 2002). Triplicate tests were performed at each test point. One test or measurement was taken with the bar parallel to the direction of compaction, the second measurement with the bar 90 degrees to the first measurement (perpendicular to the direction of compaction), and the final measurement taken 180 degrees to the first measurement. Figure 34 shows the DSPA in operation, while table 19 provides the average seismic modulus values.

GeoGauge

The Humbolt Soil Stiffness gauge (referred to as the GeoGauge in this interim report) was used to measure the resilient modulus of the unbound materials in accordance with the procedure recommended by the manufacturer – with one exception. The test was performed with and without a sand cushion below the plate on selected projects (SH-12, TH-23, and US-280), because one of the agencies that hosted a project had been using the gauge without a sand cushion.



(a) View of the DSPA.



(b) Field testing using the DSPA.

Figure 34 Dirt Seismic Pavement Analyzer Tests on US-280 Base layer.

Table 19 – Summary of the Seismic Modulus Measured from the DSPA Test Results, ksi

Project ID	Area	A	B	C	D
I-85 Low Plasticity Clay; Section 1, Before IC Rolling	Mean	26.2	31.8	27.9	34.2
	COV, %	28.4	7.7	14.1	20.9
I-85 Low Plasticity Clay; Section 2, Before IC Rolling	Mean	24.1	27.2	38.3	44.4
	COV, %	22.9	23.9	9.6	21.7
I-85 Low Plasticity Clay; Section 1, After IC Rolling	Mean	42.5	38.7	37.0	39.5
	COV, %	5.9	22.4	20.0	21.8
I-85 Low Plasticity Clay; Section 2, After IC Rolling	Mean	33.2	39.7	45.1	43.7
	COV, %	12.8	27.6	10.7	25.8
SH-21 High Plasticity Clay; Area 2, No IC Rolling	Mean	---	---	---	23.6
	COV, %	---	---	---	7.6
SH-21 High Plasticity Clay; Area 1, With IC Rolling	Mean	25.8	25.0	30.4	---
	COV, %	18.1	11.3	11.5	---
TH-23 Embankment, Silt-Sand-Gravel Mix; South Section	Mean	42.00	45.13	31.12	---
	COV, %	14.5	20.8	43.9	---
TH-23 Embankment, Silt-Sand-Gravel Mix; North Section	Mean	51.66	40.20	31.13	---
	COV, %	23.2	23.4	29.7	---
SH-130 Granular, Improved Embankment; Section 1	Mean	38.4	39.0	34.4	---
	COV, %	9.0	23.0	22.1	---
SH-130 Granular, Improved Embankment; Section 2	Mean	33.5	38.5	35.3	---
	COV, %	33.1	27.5	18.8	---
SH-130 Granular, Improved Embankment; Section 3	Mean	29.9	26.7	30.1	---
	COV, %	15.8	21.1	6.6	---
TH-23 Crushed Aggregate; North Section	Mean	71.87	119.9	61.4	---
	COV, %	41.2	40.4	43.0	---
TH-23 Crushed Aggregate; Middle Section	Mean	89.47	69.67	28.0	---
	COV, %	79.7	48.6	37.2	---
TH-23 Crushed Aggregate; South Section	Mean	112.8	108.6	62.8	---
	COV, %	71.4	41.1	53.2	---
US-280 Crushed Stone, Section 1	Mean		233.5		---
	COV, %		13.8		---
US-280 Crushed Stone; Section 2	Mean		189.0		---
	COV, %		22.0		---
US-280 Crushed Stone; Section 3	Mean		173.2		---
	COV, %		16.2		---
US-280 Crushed Stone; Section 4	Mean		117.4		---
	COV, %		12.8		---

Note: The shaded cells designate those areas with anomalies (refer to table 14); black cells denote weaker areas, while the gray cells denote stronger areas tested within a specific project.

The sand cushion did make a difference in the measured values for some materials. The resilient modulus values were found to be greater when using the sand cushion on rough surfaces, similar to a crushed aggregate or granular base. A ratio of approximately 2.2 was determined between the two conditions. This ratio or difference (modulus measured with and without a sand cushion) decreased on fine-grained surfaces. In fact, no systematic difference (ratio equal to 1.0) was detected on the SH-21 project with high plasticity clay soil. For consistency, however, the sand cushion is recommended for use in all future testing.

Figure 35 shows the GeoGauge in operation, prior to placing the sand cushion, while table 20 summarizes the average resilient modulus values measured within each section for the projects where the GeoGauge was used.



Figure 35 GeoGauge used for stiffness testing on all unbound materials.

Triplicate tests were performed at each test point. The gauge was placed and seated on the surface by applying a slight pressure and rotation to ensure uniform contact – making sure that the surface and gauge were coupled. The gauge was then lifted and this sequence repeated.

Table 20 – Summary of the Resilient Modulus Values Measured with the GeoGauge, ksi					
Project ID	Area	A	B	C	D
I-85 Low Plasticity Clay; Section 1, Before IC Rolling	Mean	14.5	16.3	14.9	15.7
	COV, %	20.7	7.4	19.2	12.2
I-85 Low Plasticity Clay; Section 2, Before IC Rolling	Mean	10.6	15.9	17.1	18.1
	COV, %	26.9	15.7	7.7	20.8
I-85 Low Plasticity Clay; Section 1, After IC Rolling	Mean	17.43	16.35	16.633	17.85
	COV, %	11.7	---	27.5	---
I-85 Low Plasticity Clay; Section 2, After IC Rolling	Mean	18.42	18.50	19.64	19.4
	COV, %	7.6	---	0.4	---
SH-21 High Plasticity Clay; Area 2, No IC Rolling	Mean	---	---	---	19.6
	COV, %	---	---	---	6.3
SH-21 High Plasticity Clay; Area 1, After IC Rolling	Mean	24.0	24.7	20.1	---
	COV, %	15.5	24.8	11.5	---
TH-23 Embankment, Silt-Sand-Gravel Mix; South Section	Mean	10.07	10.86	7.537	---
	COV, %	10.2	11.0	9.4	---
TH-23 Embankment, Silt-Sand-Gravel Mix; North Section	Mean	12.568	10.00	10.31	---
	COV, %	15.6	4.5	22.0	---
SH-130 Granular, Improved Embankment; Section 1	Mean	28.74	26.82	27.72	---
	COV, %	14.2	15.3	9.0	---
SH-130 Granular, Improved Embankment; Section 2	Mean	22.92	26.71	25.21	---
	COV, %	17.5	14.4	21.2	---
SH-130 Granular, Improved Embankment; Section 3	Mean	24.62	22.97	19.21	---
	COV, %	7.7	1.5	17.2	---
TH-23 Crushed Aggregate; North Section	Mean	13.64	15.16	12.374	---
	COV, %	11.1	10.2	9.1	---
TH-23 Crushed Aggregate; Middle Section	Mean	12.97	12.55	9.838	---
	COV, %	25.0	15.8	17.6	---
TH-23 Crushed Aggregate; South Section	Mean	15.64	14.37	11.718	---
	COV, %	24.3	14.5	16.2	---
US-280 Crushed Stone; Section 1	Mean		48.84		---
	COV, %		7.9		---
US-280 Crushed Stone; Section 2	Mean		49.98		---
	COV, %		5.0		---
US-280 Crushed Stone; Section 3	Mean		44.96		---
	COV, %		9.9		---
US-280 Crushed Stone; Section 4	Mean		35.12		---
	COV, %		4.6		---

Note: The shaded cells designate those areas with anomalies (refer to table 14); black cells denote weaker areas, while the gray cells denote stronger areas tested within a specific project.

Comparison of Test Results from Seismic Based Devices

Figure 36 compares the seismic and resilient modulus values measured with this technology. As shown, the seismic modulus values measured with the DSPA are greater than the resilient modulus values measured with the GeoGauge. The difference between the two values increases with stiffer and coarser materials. However, there is correspondence between the two seismic devices. In fact, the DSPA or GeoGauge values can be adjusted to result in similar values (refer to section 3.2.2 – Adjustment of Field Results).

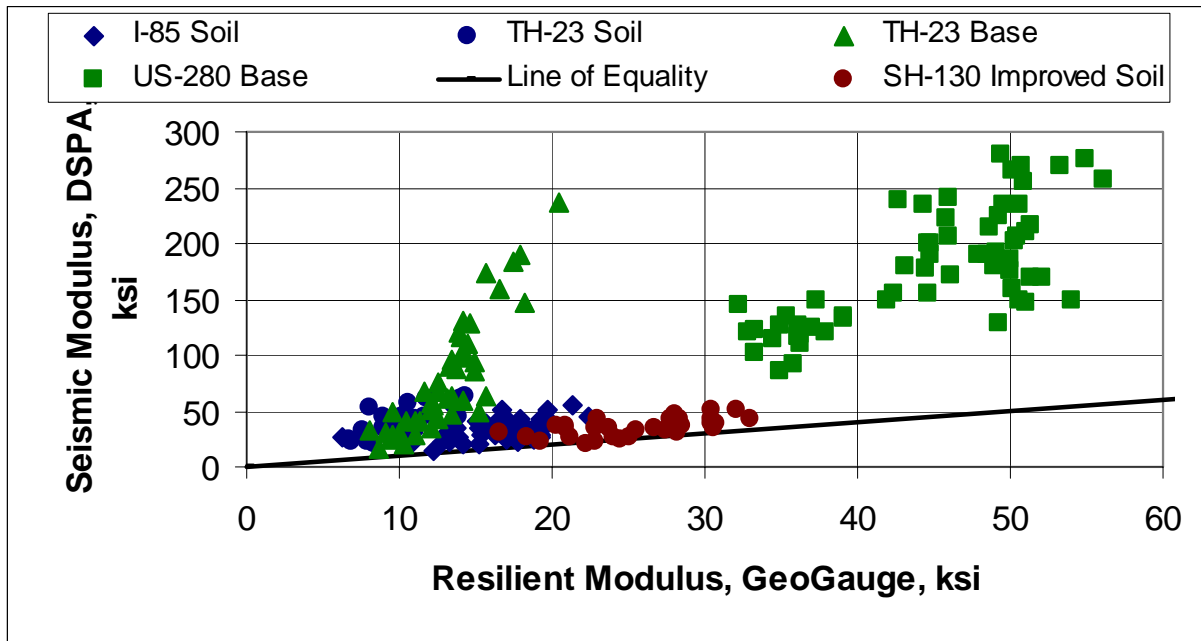
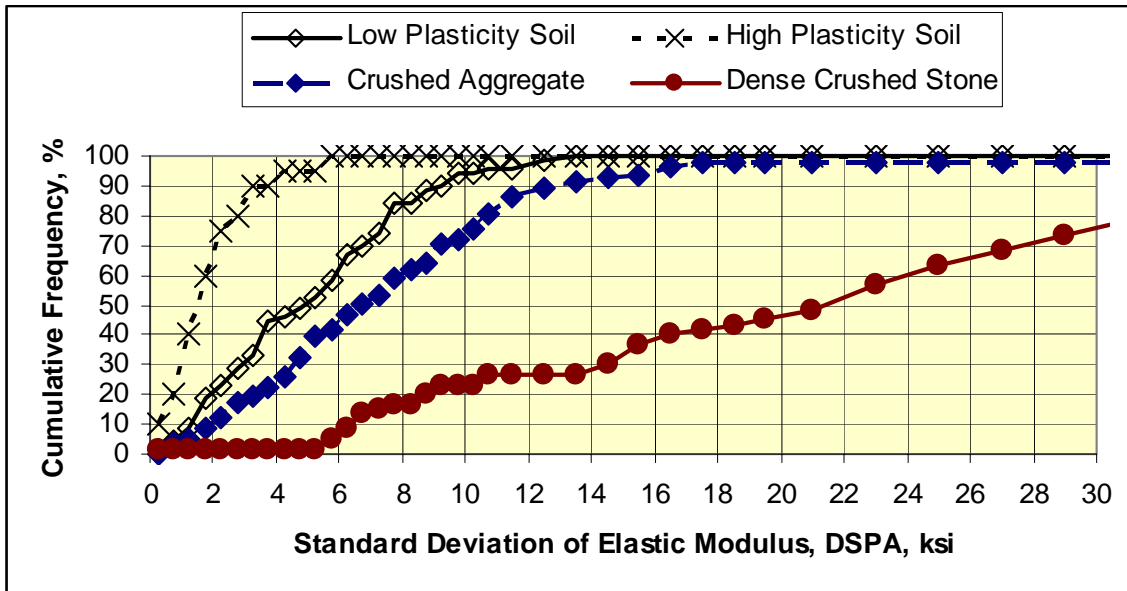


Figure 36 Comparison of the seismic modulus values measured with the DSPA and resilient modulus values measured with the GeoGauge.

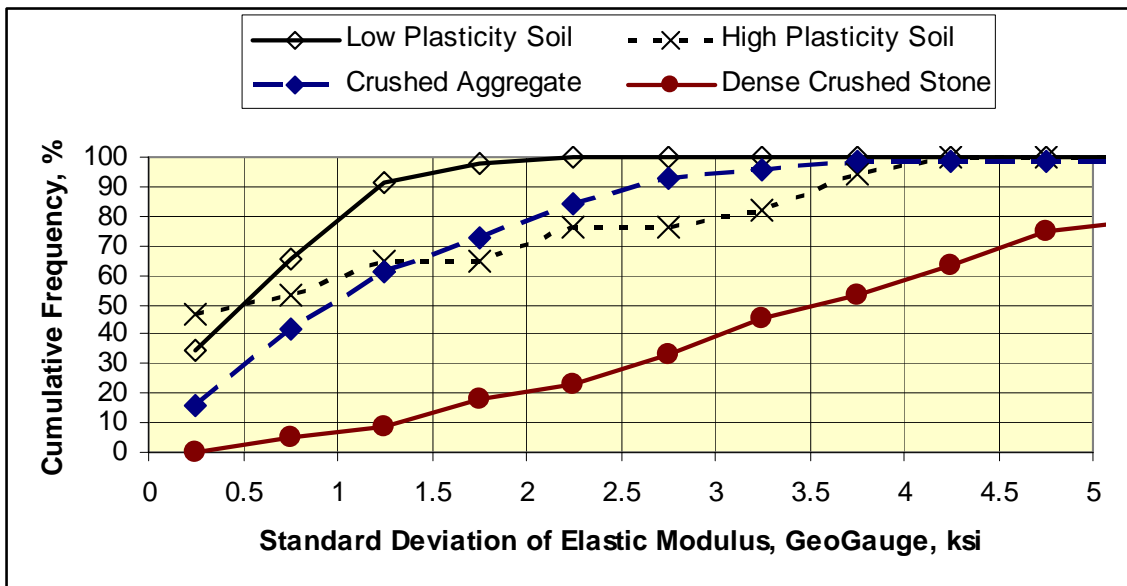
Figure 37 presents a cumulative frequency diagram of the standard deviation or repeatability of the DSPA and GeoGauge. The standard deviations in figure 37 represent the triplicate measurements taken at the same test point. The variability of measurements made with the DSPA (figure 37.a) is higher than for the GeoGauge (figure 37.b), especially for the stiffer and coarse-grained materials. The repeatability of the GeoGauge devices is considered good, but is material dependent. The mean standard deviation of the GeoGauge varies from about 0.5 ksi for the weaker soils to 3.5 ksi for dense base materials. The DSPA has a mean standard deviation varying from about 1.5 ksi to over 21 ksi.

A reason for the higher variability of the DSPA was the rotation of the sensor bar relative to the roller direction. The GeoGauge was not rotated between repeat readings because of the circular loading plate. Another reason for the higher variability is that the DSPA measures the stiffness of the upper 6 inches, while the GeoGauge and other NDT devices (excluding the DCP) can be influenced by the supporting layers. More importantly, the moisture gradient is much greater nearer the surface which has a greater influence on those devices

that measure material responses closer to the surface – the DSPA. Thus, the mean seismic modulus values and variance of those values are higher.



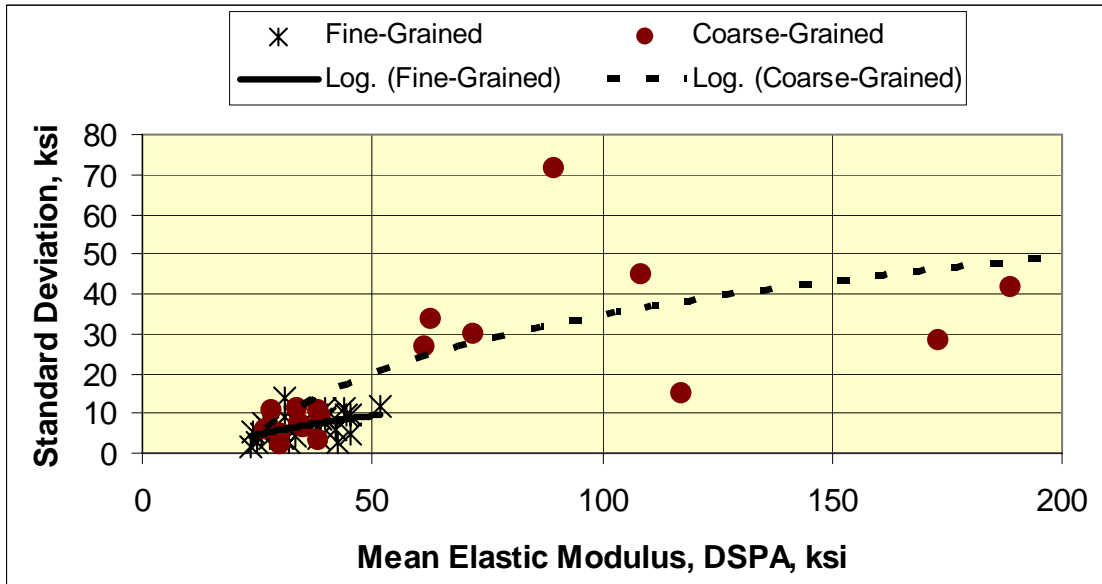
(a) Standard deviation or repeatability for the DSPA.



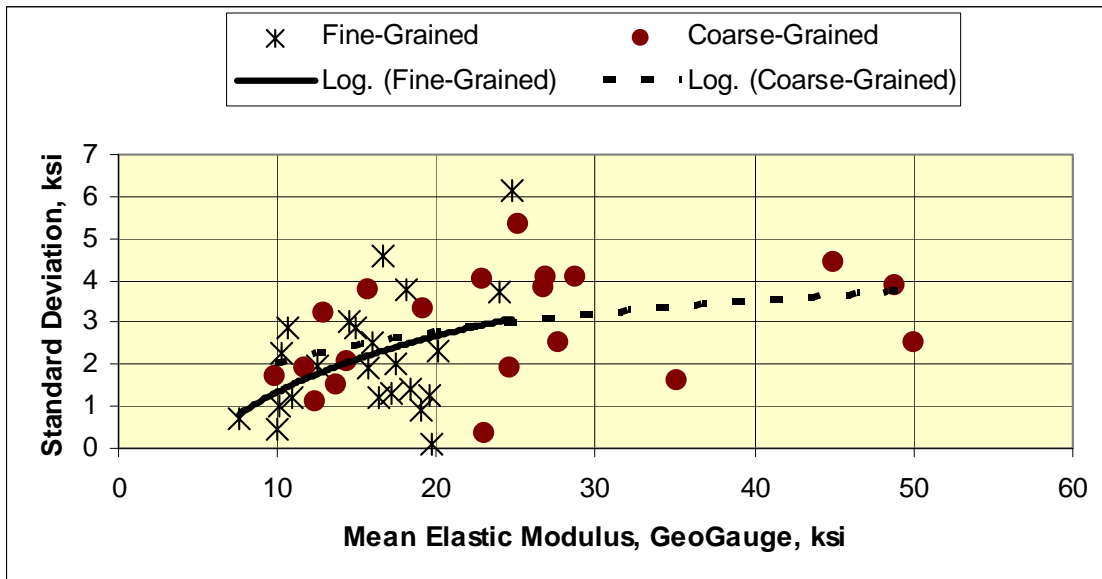
(b) Standard deviation or repeatability for the GeoGauge.

Figure 37 Cumulative frequency of the standard deviation from the seismic devices.

Figure 38 compares the standard deviation to the mean of the elastic modulus values determined from the seismic methods for different unbound materials. The standard deviation of the DSPA (figure 38.a) and GeoGauge (figure 38.b) slightly increases with increasing elastic modulus values. Figure 38.a does not show all of the DSPA data – it only shows the mean elastic modulus values less than 200 ksi for visual comparison to the other NDT devices.



(a) Standard deviations from the DSPA for all projects; mean elastic modulus values greater than 100 ksi are not shown in the graph.



(b) Standard deviations from the GeoGauge for all projects.

Figure 38 Standard deviations of the elastic modulus values resulting from the seismic-based methods for testing unbound materials.

Contrary to the findings from the DCP and deflection-based methods, both the DSPA and GeoGauge found that the elastic modulus values of fine and coarse-grained materials were within the same range for many of the test sections. This difference between the different technologies will be discussed in greater detail in section 3.4.1.

Figure 39 compares the coefficient of variations determined in different areas of a project with each device. In general, the GeoGauge was found to have the lower variability in modulus values. The coefficient of variation in the TH-23 crushed aggregate base modulus values from the DSPA tests was found to be high. The reason for the high variation is unknown. However, the moisture gradient could be higher along this project, because of rains that occurred prior to NDT testing.

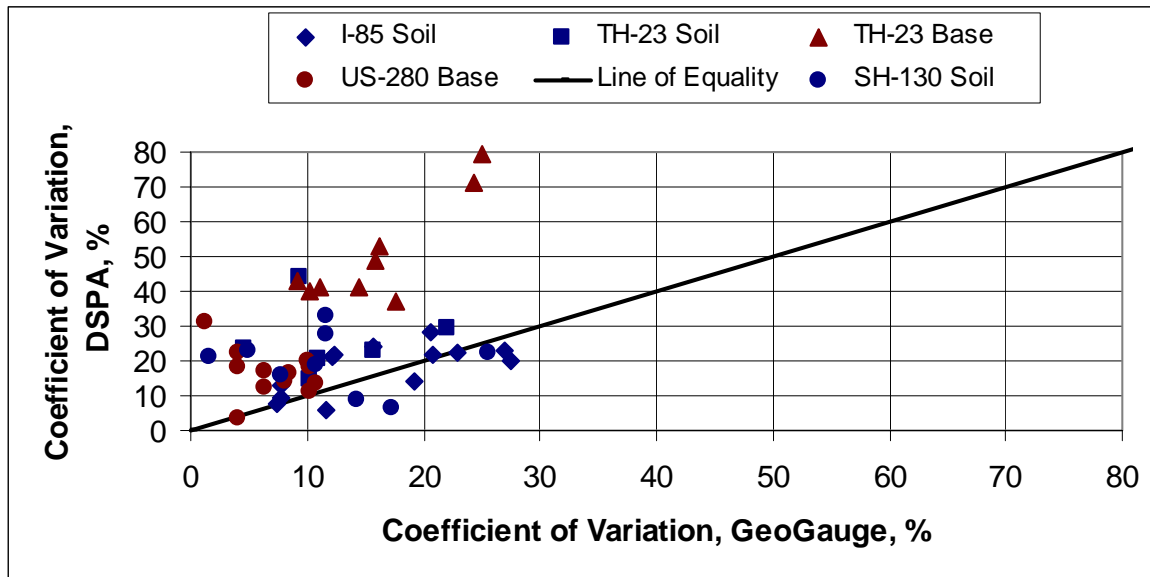


Figure 39 Comparison of the coefficient of variations of the modulus values measured with the DSPA and GeoGauge.

The cells in tables 19 and 20 that correspond to those conditions listed in table 14 have been shaded. The following bullets summarize the results of the seismic tests in accordance with those conditions listed in table 14.

- I-85 Low Plasticity Soil Embankment – Both seismic devices found lane A of section 2 to be the weakest, prior to IC rolling. This is the area where thicker lifts had been placed. The seismic results also indicate an increase in the embankment’s strength after IC rolling, but not a reduction in stiffness variability.
- SH-21 High Plasticity Clay – Both seismic devices found section 2 to be slightly weaker than section 1, which is consistent with construction records. Both devices showed a slight benefit when using the IC roller for testing and compaction.
- TH-23 Gravelly, Silty Clay Embankment – Both NDT devices correctly found lane C of the south section to be the softer (less stiff) of the areas tested, and found lane A of the north section to be stronger.

- SH-130 Improved Granular Embankment – The GeoGauge did not detect any difference between the three areas tested, while the DSPA found section 3 to be consistently weaker, which was not planned.
- TH-23 Crushed Aggregate Base – Both NDT devices found that lane C of the middle section was weaker, and lane A of the south section was the stronger of the areas tested, which is consistent with construction records.
- US-280 Crushed Stone Base – Both seismic devices found area 4 to be weaker of the four areas tested. However, its strength is still high and consistent with adequately compacted crushed stone, similar to the findings with the DCP.

3.1.4 Ground Penetrating Radar Testing

A ground penetrating radar (GPR), single air-coupled antenna was used to take dielectric measurements of the unbound materials in accordance with ASTM and the procedure outlined by Maser and others (Maser, et al., 2003). Triplicate runs were made for each line of points within a section. Figure 7 in Chapter 2 showed the GPR in operation. Table 21 summarizes the average dielectric values measured at each test point for the other NDT devices for comparison purposes.

One of the key advantages of the GPR is that a continuous profile of the dielectric values can be measured – in contrast to point-based devices. Contours of the dielectric measurements were prepared and used to determine the values at specific points where other tests were performed. Obviously, the increased sampling error between repeat runs will increase the overall variability of the GPR point measurements. Where the measurement lanes were well defined, the coefficient of variation (COV) of the dielectric values was significantly less than for the wider areas. As an example, the COV for the I-85 embankment area was as high as 50 percent, while the COV along the narrow US-280 test lane never exceeded 12 percent (refer to table 21).

Density contours and profiles were also prepared for each layer. Figures 40 and 41 present examples of contours that were prepared from the dielectric readings. Wet densities were calculated from these dielectric values, assuming a moisture content for the unbound materials in a specific area. Figure 42 shows an example of the density profile for the TH-23 crushed aggregate base material.

The wet densities were found to be highly variable and generally did not coincide with the actual densities measured from the sand cones and nuclear density gauge readings. As an example, the following lists the average densities (pcf) that were estimated from the GPR data for the crushed aggregate base material placed along the TH-23 project in Minnesota.

Lane	A	B	C	Comment
North Section	---	129.2	142.4	
Middle Section	---	130.8	150.6	Lane C had the less dense base.
South Section	---	131.0	145.8	Lane A & B had the denser base.



Conversely, all other NDT devices found lanes A and B to be stronger than lane C (tables 15, 17, 19, and 20). In general, the GPR did not adequately identify those areas with anomalies. As noted above, a reason for this observation is that the moisture content for a particular area was assumed to be constant to identify changes in density, and vice-versa for moisture content. Another reason is that the anomaly may have been caused by variations in gradation and other physical properties that would be difficult, at best, to identify with the GPR.

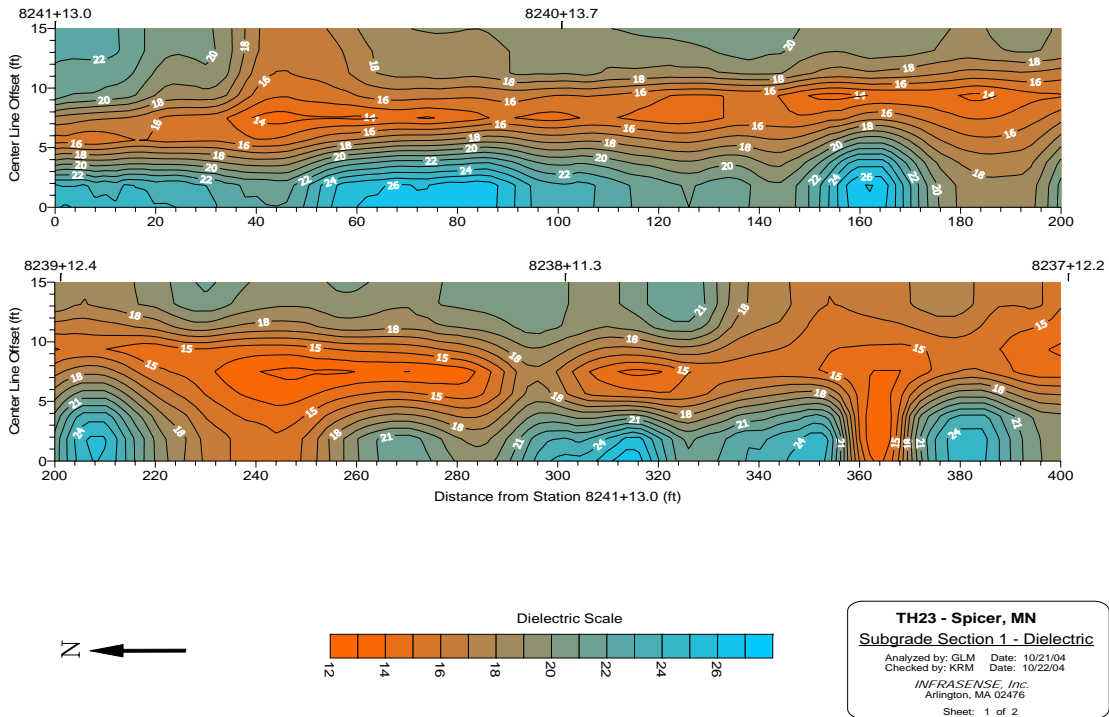
Layer thickness was also determined from the GRP test results, and concurred with the thickness reported during construction. The thicknesses resulting from the GPR are provided in the appendices. Figure 43 presents an example of the thickness profiles (crushed aggregate base layer for the TH-23 reconstruction project) that were prepared from the dielectric readings.

Table 21 – Summary of the Dielectric Values Measured with GPR on the Unbound Layers

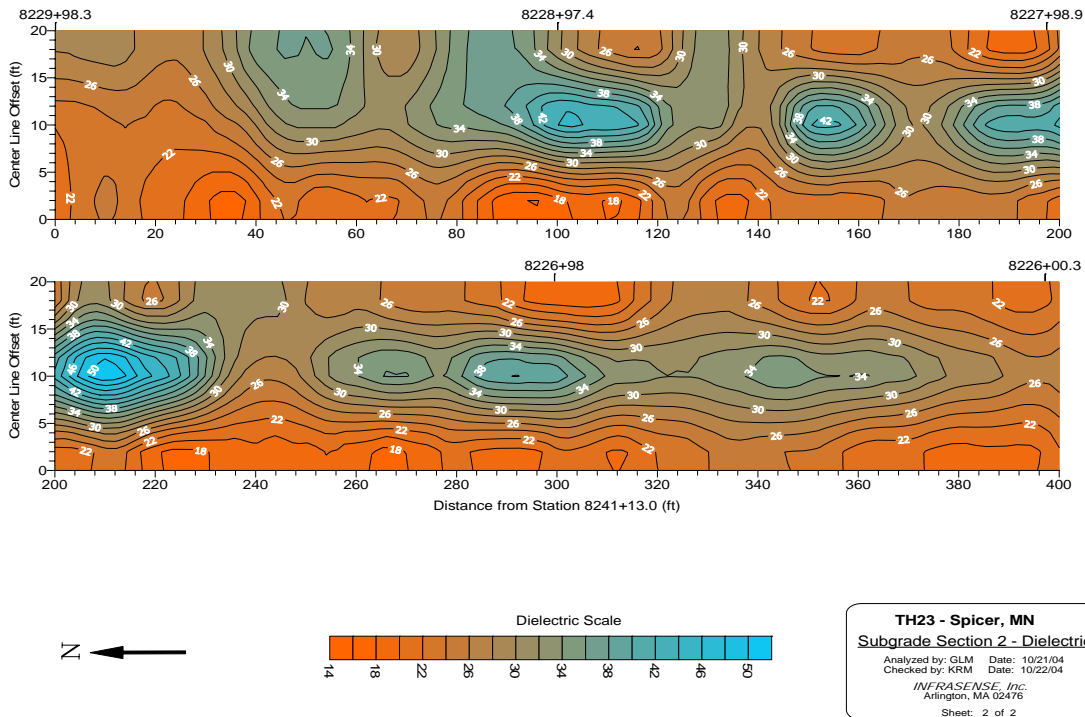
Project ID	Area	A	B	C	D
I-85 Embankment, Silty Clay; Section 1, Before Rolling	Mean	15.38	15.79	14.29	15.19
	COV, %	17.8	23.3	53.6	25.7
I-85 Embankment, Silty Clay; Section 2, Before IC Rolling	Mean	13.91	17.47	16.82	16.38
	COV, %	29.0	20.5	30.7	24.1
I-85 Embankment, Silty Clay; Section 1, After IC Rolling	Mean	20.37	21.23	21.61	23.23
	COV, %	15.8	10.6	15.0	12.6
I-85 Embankment, Silty Clay; Section 2; After IC Rolling	Mean	19.13	23.75	23.77	25.36
	COV	10.2	10.7	17.6	8.4
TH-23 Embankment, Silt-Sand-Gravel Mix; South Section	Mean	23.004	13.468	19.334	---
	COV, %	11.3	7.0	14.4	---
TH-23 Embankment, Silt-Sand-Gravel Mix; North Section	Mean	20.324	34.438	23.882	---
	COV, %	22.2	32.7	22.7	---
SH-130 Improved Embankment; Section 1	Mean	9.225	10.00	7.65	---
	COV	33.1	42.3	42.9	---
SH-130 Improved Embankment; Section 2	Mean	12.875	8.875	9.825	---
	COV	90.3	47.4	20.1	---
SH-130 Improved Embankment; Section 3	Mean	8.775	9.025	11.85	---
	COV, %	51.5	50.8	48.7	---
TH-23 Crushed Aggregate; North Section	Mean	---	8.796	10.042	---
	COV, %	---	1.6	5.4	---
TH-23 Crushed Aggregate; Middle Section	Mean	---	8.950	10.87	---
	COV, %	---	6.1	10.9	---
TH-23 Crushed Aggregate; South Section	Mean	---	9.792	10.378	---
	COV, %	---	8.2	4.3	---
US-280 Crushed Stone; Section 1	Mean		11.723		
	COV, %		8.3		
US-280 Crushed Stone; Section 2	Mean		12.222		
	COV, %		11.4		
US-280 Crushed Stone; Section 3	Mean		11.919		
	COV, %		7.3		
US-280 Crushed Stone; Section 4	Mean		11.569		
	COV, %		7.0		

Notes:

- The shaded cells designate those areas with anomalies (refer to table 14); the black cells denote the weaker areas, while the gray cells denote the stronger areas tested within a specific project.
- Due to construction sequencing, lane A of the TH-23 crushed aggregate base sections could not be tested with the GPR after it arrived on site.

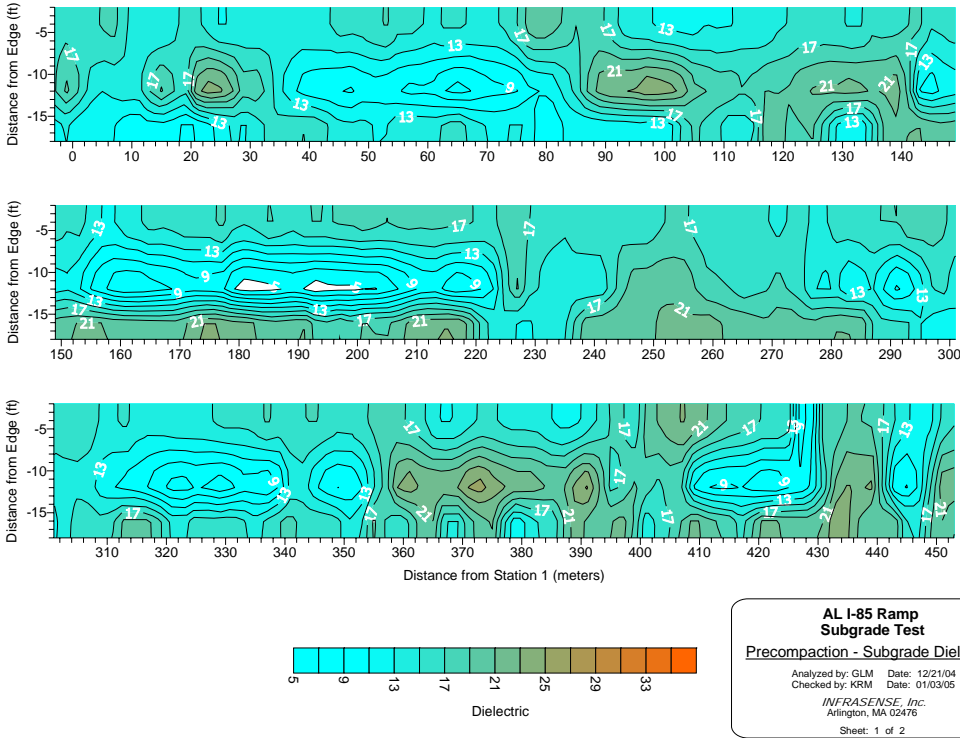


(a) Section 1 of the Embankment.

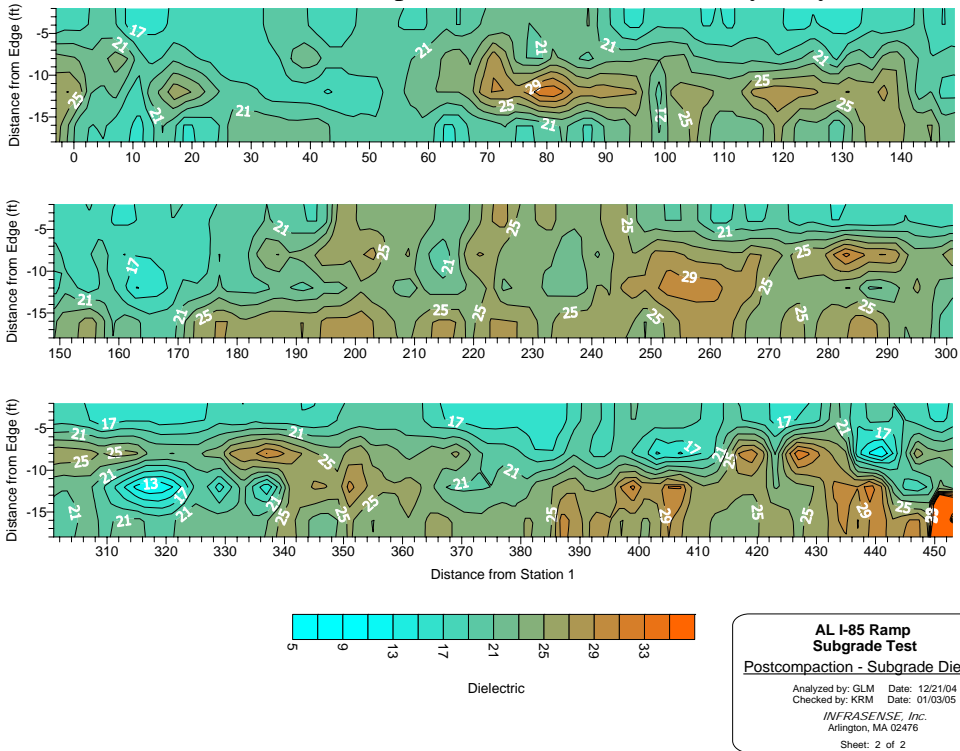


(b) Section 2 of the Embankment.

Figure 40 Example: Dielectric contours generated from the GPR test results for the gravelly-silty clay embankment placed along the TH-23 reconstruction project.



(a) Pre-IC Compaction of the Low Plasticity Clay Embankment.



(b) Post-IC Compaction of the Low Plasticity Clay Embankment.

Figure 41 Example: Dielectric contours generated from the GPR test results for the low plasticity soil embankment placed on the I-85 exit ramp reconstruction project.

Figure 42 Example: Density profiles generated from the GPR test results for the crushed aggregate base layer placed along the TH-23 reconstruction project.

Figure 43 Example: Thickness profiles generated from the GPR test results for the crushed aggregate base layer placed along the TH-23 reconstruction project.

3.1.5 Non-Nuclear Density Testing

The non-nuclear, Electrical Density Gauge (EDG) was used to measure the density and moisture content of the unbound materials placed along each project. Figure 44 shows the EDG and its setup for measuring the density and moisture content in unbound materials. The test was performed in accordance with the manufacturer's recommendations.

Triplicate readings were made at each test point without moving the 6-inch probes. The EDG measurements made at each test point were adjusted based on calibration densities obtained from sand cones or nuclear density readings that were suppose to cover the range of values expected for the project. A soil model was developed for each unbound material and that soil model was used to determine the actual densities and moisture contents from the EDG readings. The accuracy of the EDG, as for the GPR, is heavily dependent on the calibration values obtained from other test results. Any error in density or moisture content from these other tests is included in the EGD values.



Figure 44 Electrical density gauge testing used on the unbound materials.



Table 22 summarizes the average dry density, while table 23 provides the average moisture content measured within each section where the EDG was used. The amount of deviation in the test results was found to be small. The COV of the density readings were generally less than 1 percent, and less than 5 percent for moisture content readings. The moisture contents listed in table 23 are generally below the optimum values obtained from construction records and measured in the laboratory. Based on observations at each site, it is expected that the moisture content of the upper layer materials are less than the optimum values for most of the areas tested, with the exception of the I-85 embankment material.

Table 24 summarizes the maximum dry densities and optimum moisture contents recovered from construction records in comparison to the average values measured along the project. In some cases, multiple moisture-density (M-D) relationships exist for a single layer within the same project. The values included in table 24 represent the M-D curve for the material nearest the location of the specific test section.

The cells in tables 22 and 23 that correspond to those conditions listed in table 14 have been shaded. The following bullets summarize the results of the EDG tests in accordance with those conditions listed in table 14.

- I-85 Low Plasticity Soil Embankment –No difference in moisture content was detected by the EDG between all areas tested. The EDG found both outside lanes to be less dense prior to and after IC rolling, similar to the DCP test results. The variation in dry density and moisture content, as measured by the EDG was found to be low.
- TH-23 Gravelly, Silty Clay Embankment – Higher moisture contents and lower dry densities were measured in the south section, but not along lane C. Lane C had the greater variability in moisture content. The variability of the dry density was found to be low.
- SH-130 Improved Granular Embankment – The EDG found no significant difference in density and moisture content between all areas tested, which was planned.
- TH-23 Crushed Aggregate Base – The EDG found no significant difference in density and moisture content between all areas tested, which is inconsistent with construction records.
- US-280 Crushed Stone Base – The EDG found no significant difference in density and moisture content between all areas tested, also inconsistent with construction records.

Table 22 – Summary of the Dry Densities Measured with the Electrical Density Gauge, pcf

Project ID	Area	A	B	C	D
I-85 Embankment, Silty Clay; Section 1, Before IC Rolling	Mean	107.92	108.9	108.6	107.7
	COV, %	1.3	0.5	1.1	1.7
I-85 Embankment, Silty Clay; Section 2; Before IC Rolling	Mean	107.2	107.5	108.9	107.2
	COV, %	0.8	0.8	1.1	1.9
I-85 Embankment, Silty Clay; Section 1, After IC Rolling	Mean	108.1	108.2	108.5	108.4
	COV, %	1.0	0.5	0.7	0.3
I-85 Embankment, Silty Clay;	Mean	107.4	107.7	108.0	107.6



Section 2, After IC Rolling	COV	0.5	0.5	0.8	1.3
TH-23 Embankment, Silt-Sand-Gravel Mix; North Section	Mean	123.9	123.7	124.4	---
	COV, %	0.4	0.1	1.0	---
TH-23 Embankment, Silt-Sand-Gravel Mix; South Section	Mean	122.5	122.9	122.9	---
	COV, %	1.8	1.8	0.8	---
SH-130 Improved Embankment; Section 1	Mean	123.7	123.7	124.9	---
	COV	0.3	0.1	0.6	---
SH-130 Improved Embankment; Section 2	Mean	122.6	123.1	122.7	---
	COV	2.0	2.0	0.8	---
SH-130 Improved Embankment; Section 3	Mean	123.3	122.3	123.7	---
	COV, %	1.4	0.1	0.2	---
TH-23 Crushed Aggregate; North Section	Mean	129.9	129.8	129.8	---
	COV, %	0	0	0	---
TH-23 Crushed Aggregate; Middle Section	Mean	129.8	129.8	129.8	---
	COV, %	0	0	0	---
TH-23 Crushed Aggregate; South Section	Mean	129.8	129.9	129.8	---
	COV, %	0.1	0.1	0	---
US-280 Crushed Stone; Section 1	Mean	147.4			
	COV, %	0.7			
US-280 Crushed Stone; Section 2	Mean	148.8			
	COV, %	0.3			
US-280 Crushed Stone; Section 3	Mean	145.9			
	COV, %	0.5			
US-280 Crushed Stone; Section 4	Mean	148.2			
	COV, %	0.3			

Note: The shaded cells designate those areas with anomalies (refer to table 14); the black cells denote the weaker areas, while the gray cells denote the stronger areas tested within a specific project.

Table 23 – Summary of the Moisture Contents Measured with the Electrical Density Gauge, percent

Project ID	Area	A	B	C	D
I-85 Embankment, Silty Clay; Section 1, Before IC Rolling	Mean	16.9	16.8	16.9	16.9
	COV, %	0.8	0.3	0.3	1.0
I-85 Embankment, Silty Clay; Section 2; Before IC Rolling	Mean	16.9	16.9	16.8	17.0
	COV, %	0.7	0.3	0.3	1.5
I-85 Embankment, Silty Clay; Section 1, After IC Rolling	Mean	16.9	16.9	16.9	16.9
	COV, %	0.5	0.3	0.4	0
I-85 Embankment, Silty Clay; Section 2, After IC Rolling	Mean	17.0	16.9	16.9	16.9
	COV	0.5	0.3	0	0.7
TH-23 Embankment, Silt-Sand- Gravel Mix; North Section	Mean	8.0	8.0	7.6	
	COV, %	5.1	1.1	11.9	
TH-23 Embankment, Silt-Sand- Gravel Mix; South Section	Mean	9.8	8.7	7.6	
	COV, %	7.5	7.3	15.8	
SH-130 Improved Embankment; Section 1	Mean	8.1	8.05	7.23	
	COV	4.4	1.2	6.8	
SH-130 Improved Embankment; Section 2	Mean	8.85	8.43	8.7	
	COV	19.8	21.6	8.4	
SH-130 Improved Embankment; Section 3	Mean	8.35	9.1	8.05	
	COV, %	14.4	1.6	0.9	
TH-23 Crushed Aggregate; North Section	Mean	4.26	4.28	4.34	
	COV, %	1.3	1.0	2.1	
TH-23 Crushed Aggregate; Middle Section	Mean	4.24	4.28	4.30	
	COV, %	1.3	2.0	1.6	
TH-23 Crushed Aggregate; South Section	Mean	4.18	4.18	4.38	
	COV, %	3.9	3.9	1.0	
US-280 Crushed Stone; Section 1	Mean		3.92		
	COV, %		3.1		
US-280 Crushed Stone; Section 2	Mean		4.18		
	COV, %		2.9		
US-280 Crushed Stone; Section 3	Mean		3.77		
	COV, %		2.9		
US-280 Crushed Stone; Section 4	Mean		4.06		
	COV, %		2.6		

Note: The shaded cells designate those areas with anomalies (refer to table 14); the black cells denote weaker areas, while the gray cells denote the stronger areas tested within a specific project.

Table 24 – Listing of the Maximum Dry Density and Optimum Moisture Content for Each Unbound Material, as Compared to the Average Test Results from the EDG

Project	Material	Maximum Dry Unit Weight, pcf	Optimum Moisture Content, %	Average Dry Density, pcf	Average Moisture Content, %
I-85	Low Plasticity Soil; Pre-IC	112.7	13.1	107.98	16.9
	Low Plasticity Soil; Post-IC			107.98	16.9
SH-21	High Plasticity Clay	108.0	21.9	NA	NA
SH-130	Improved Granular Embankment	122	9	123.3	8.32
TH-23	Silt-Sand-Gravel Mix – South Area	122.6	12	122.77	8.69
	Silt-Sand-Gravel Mix – North Area			123.80	7.87
TH-23	Crushed Aggregate Base	135.3	7.8	129.82	4.3
US-280	Crushed Stone Base	148.5	6.2	147.58	3.9

3.1.6 Intelligent Compaction Testing

TH-23 Base Material

The Caterpillar IC roller was used to test the Class 6 crushed aggregate base materials on the TH-23 project in Spicer, Minnesota. The IC roller (shown in figure 5 in Chapter 2) was set in low amplitude so that the roller would not decompact or damage the existing base material. Figures 45 and 46 show example print outs that were obtained from the IC roller’s instrumentation.

The stiffness responses recorded by the IC roller were about the same between both areas tested. Based on the interpretation of the readings by the operator, the IC roller suggests that the crushed aggregate base material is as dense as it can be along these lanes. Further compaction could damage or decompact the aggregate base layer. The following tabulates the results from the stiffness measurements made with the IC roller, which are explained and discussed in the bullets that follow.

Area	Lanes Tested	A	B	C
1 – South Section	Mean	35.00	24.22	41.80
	Standard Deviation	9.25	9.38	6.78
	COV, %	26.4	38.7	16.2
2 – Middle Section	Mean	38.40	31.78	31.30
	Standard Deviation	13.01	8.70	5.79
	COV, %	33.9	27.4	18.5

- South Section, Area 1 (figure 45) – Lanes A and C were found to be the stiffer based on the measured responses by the IC roller. The lowest stiffness readings were recorded in the northern part of lane B. Conversely, the other NDT devices found lane C to be weaker (refer to tables 15, 17, 19, and 20).

- Middle Section, Area 2 (figure 46) – The IC roller found no consistent difference between the three lanes. The weaker area identified by the DSPA, GeoGauge, DCP, and LWD was found to be along lane C (refer to tables 15, 17, 19, and 20). Lane C has the lower densities and higher moisture contents. The IC roller may have bridged the less dense area along lane C making it difficult to detect the lower strengths.

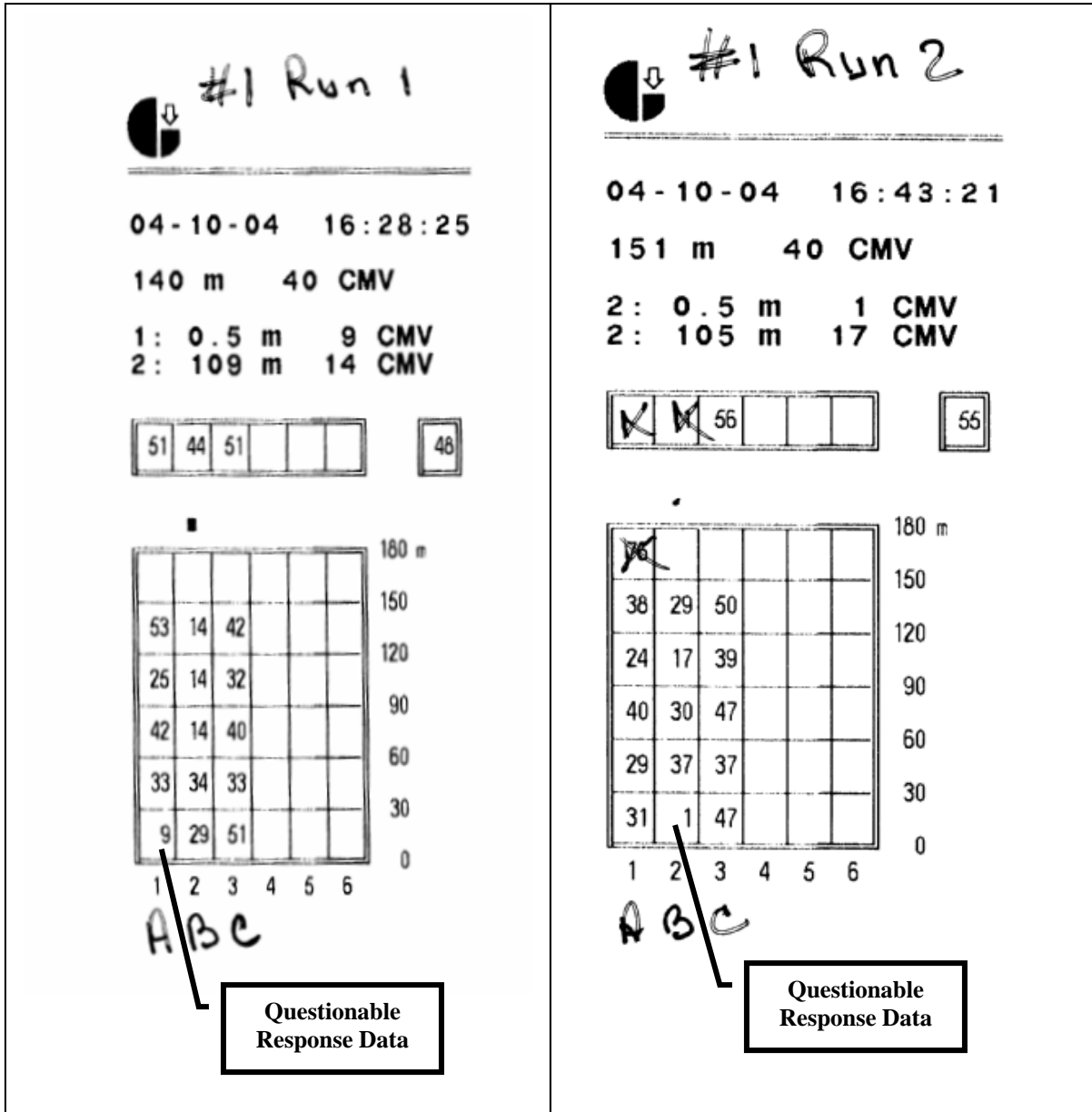


Figure 45 Print outs from the IC roller used to test the crushed aggregate base in area 1 of the TH-23 reconstruction project in Spicer, Minnesota.

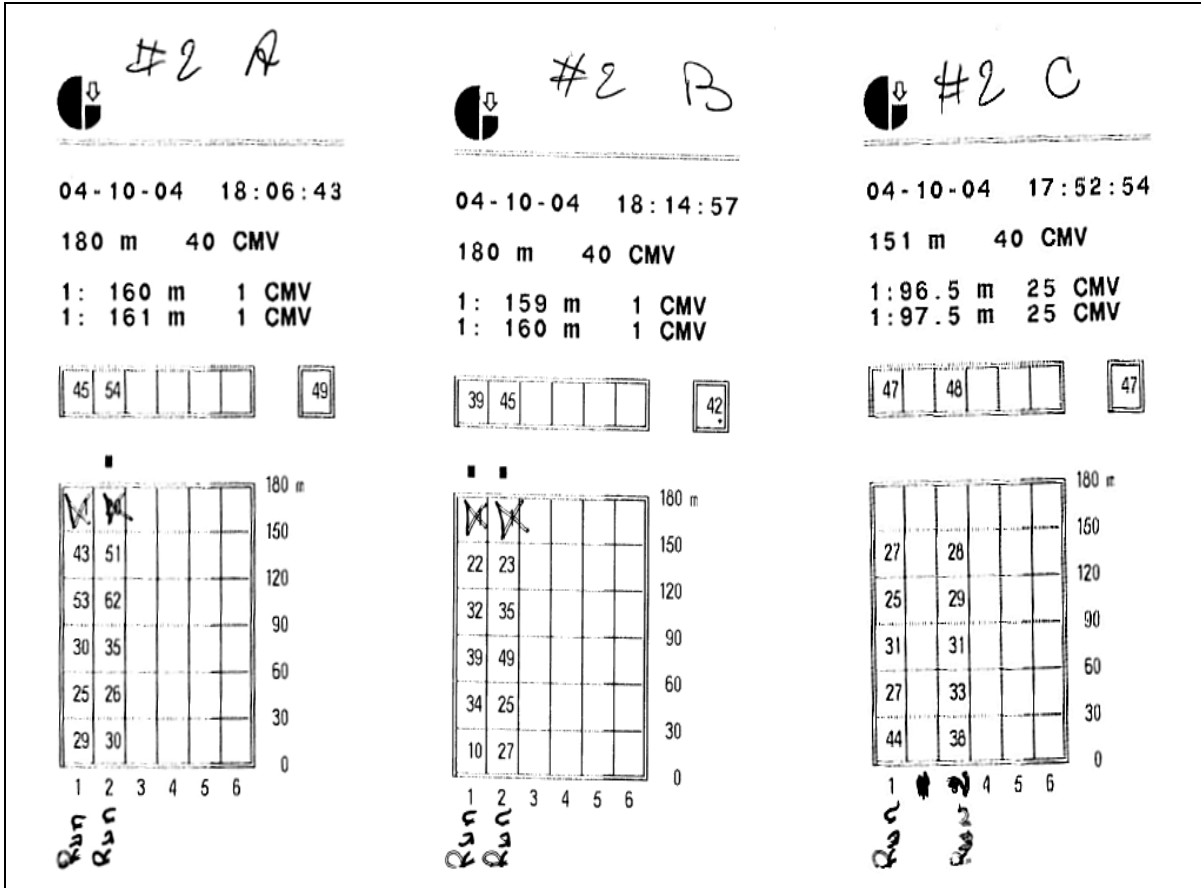


Figure 46 Print outs from the IC roller used to test the crushed aggregate base in area 2 of the TH-23 reconstruction project in Spicer, Minnesota.

I-85 Exit Ramp 51 – Embankment Material

Nondestructive testing was performed on the embankment material prior to final compaction. The Ammann IC roller was used to complete the compaction of the two embankment sections along the I-85 reconstruction of the Exit ramp 51 (refer to figure 18 in Chapter 2). After IC rolling, selected NDT devices were used to re-test each area. The results from this testing were provided in the respective tables for each NDT device, previously discussed in this chapter.

Figure 47 compares the modulus values before and after IC rolling, as measured by the GeoGauge, DSPA, and DCP devices. As shown, the modulus values consistently increased after IC rolling, with the exception of the DCP device. In general, the test results from those NDT devices suggest increases in density of the embankment. The GRP test results also show a benefit (increased density) of the additional compaction (refer to table 21). Conversely, the EDG did not show any increase in the embankment density (refer to table 22).

Figure 48 compares the coefficient of variation of those average modulus values before and after IC rolling. The variability in the modulus values did not decrease. In other words, the uniformity of the stiffness of the embankment did not significantly increase. The GPR test results, however, did show a significant reduction in variability of the dielectric values.

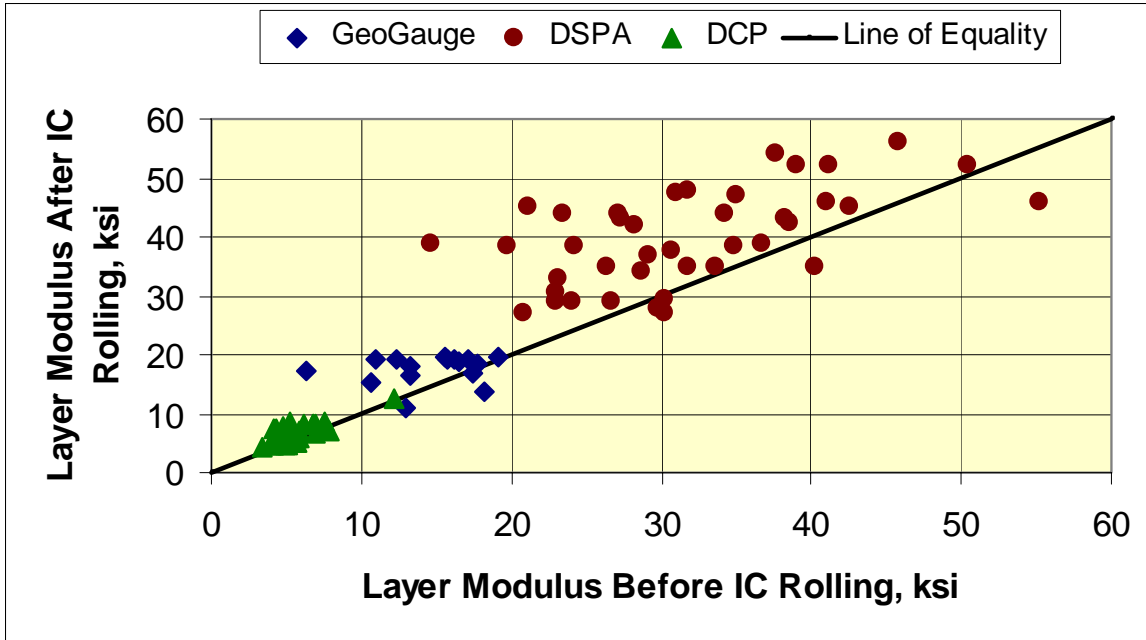


Figure 47 Comparison of modulus values measured with different NDT devices before and after IC rolling of the I-85 embankment.

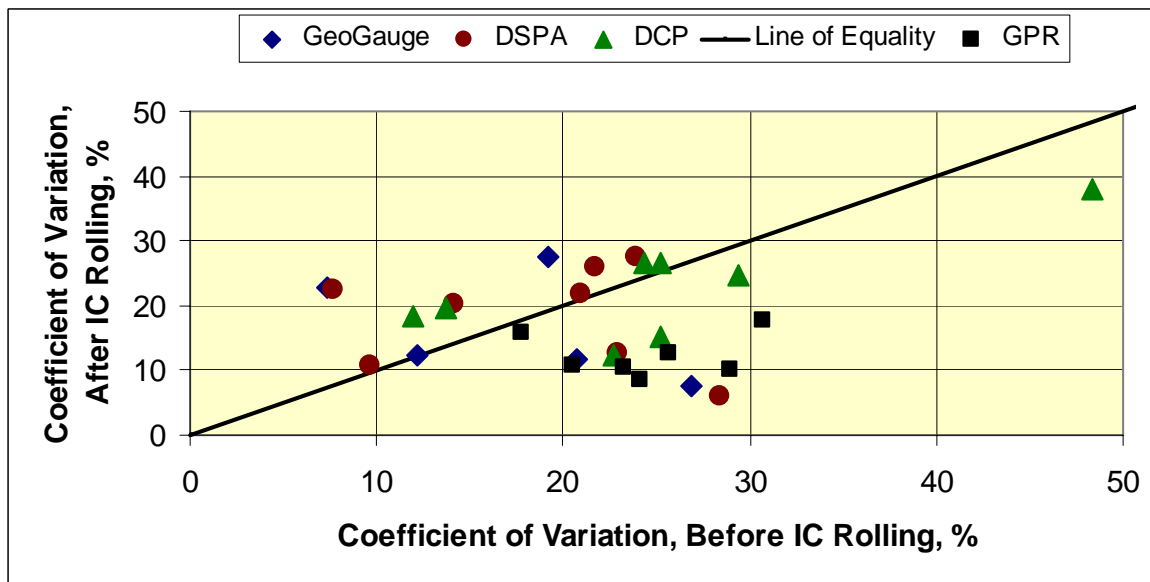


Figure 48 Uniformity of the embankment along I-85 Exit 51 before and after IC rolling, as determined through modulus measurements from different NDT devices.

3.2 Identification of Material Anomalies and Features

One of the hypotheses for the NDT technologies and devices selected for Part A of the field testing plan was to confirm that the NDT device can consistently identify anomalies or physical changes in the unbound materials (refer to table 14) that affect performance and design life of flexible pavements. A standard t-test and the Student-Newman-Keuls (SNK) mean separation procedure using a 95 percent confidence level were used to determine whether the areas with anomalies were significantly different from the other areas tested.

Table 25 tabulates the comparisons and results for checking the hypothesis. In summary, the DSPA did identify nearly all areas with anomalies. The GeoGauge did a reasonable job followed by the DCP and LWD. The EDG and GPR devices did a poor job in identifying the areas with anomalies in the unbound layers. The following summarizes the identification of the physical differences of the unbound material within a project for the NDT devices.

NDT Device	DSPA	GeoGauge	DCP	LWD	GPR	EDG
Success Rate, %	86	79	64	64	43	36

The DSPA and GeoGauge have acceptable success rates, while the EDG and GPR have unacceptable rates. More importantly, the modulus measuring devices (DSPA, GeoGauge, DCP, and LWD) found all of the hypotheses to be true for the crushed aggregate materials (TH-23 and US-280 projects), while the volumetric devices (GPR and EDG) rejected all of the hypotheses. This observation suggests systematic differences between the technologies. The following bullets summarize some of the important differences between the technologies and devices (the bullets are continued on page 73).

- The DSPA and GeoGauge induce small dynamic stress waves into the material being tested. These small responses emphasize the effect of changes in the density and moisture content of the material being tested. More importantly, both devices measure the responses in a relatively limited area and depth. In fact, the sensors for the DSPA (refer to figure 34.a) were spaced so that the response readings were confined to the upper 6 inches. The GeoGauge measurements have a deeper influence, so the test results can be influenced by the supporting layer. The depth of influence depends on the thickness and stiffness of the material being tested.
- The DCP is a point-based test and estimates the shear strength of the material from the average penetration rate through the material. The penetration rate is dependent on the dry density of the material. However, there are other physical properties that have a greater effect on the penetration rate. The amount and size of the aggregate particles can have a larger effect on the estimated modulus than for the DSPA or GeoGauge, especially for fine-grained soils with some aggregates. For example, the DCP found all of the hypotheses to be true for the coarse-grained materials and rejected many of the hypotheses for the fine-grained embankment materials with varying amounts of coarse aggregate.



Table 25. Summary on the Effectiveness of the Different NDT Devices Used to Identify Areas with and without Anomalies and with Different Physical Condition.

Project	Hypothesis		NDT Device					
			GPR	EDG, pcf	Geo., ksi	DSPA, ksi	DCP, ksi	Defl., ksi
I-85 Low Plasticity Soil Embankment	Pre-IC Rolling	Lane A	14.65	107.6	12.6	25.2	5.20	---
		Lanes B,C,D	15.99	108.1	16.3	34.0	5.62	---
	Lane A is weaker		No	Yes	Yes	Yes	No	---
	Post-IC	Area 1	21.61	108.3	17.1	39.4	6.93	9.99
		Area 2	23.00	107.7	19.0	40.4	6.21	11.78
	No Planned Difference		Yes	No	No	Yes	Yes	No
	All areas	Pre-IC	15.65	108.0	15.4	31.8	5.51	---
		Post-IC	22.31	108.0	17.7	39.9	6.57	---
Post-IC area is stronger		Yes	No	Yes	Yes	Yes	---	
SH-21 High Plasticity Clay	Area 2	No IC	---	---	19.6	23.6	11.9	---
	Area 1	With IC	---	---	22.9	27.1	9.1	---
	Area 1 is stronger		---	---	Yes	Yes	No	---
	With IC Rolling	Lane C	---	---	20.1	30.4	9.9	12.9
		Lanes A,B	---	---	24.4	25.4	8.7	8.00
	Lane C is stronger		---	---	No	Yes	No	Yes
TH-23 Silt-Sand-Gravel Mix Embankment	So. Area	Lanes A,B	18.24	122.7	10.5	43.6	15.16	5.65
	No. Area	Lanes B,C	29.16	124.1	10.1	35.7	19.01	4.77
	No Planned Difference		No	No	Yes	No	No	No
	So. Area	Lane C	19.33	122.9	7.5	31.1	11.47	5.58
		Lanes A,B	18.24	122.7	10.5	43.6	15.16	5.65
	Lane C is weaker		No	No	Yes	Yes	Yes	No
	No. Area	Lane A	20.32	123.9	12.6	51.7	18.52	4.69
		Lanes B,C	29.16	124.1	10.1	35.7	19.01	4.77
Lane A is stronger		No	No	Yes	Yes	No	No	
SH-130 Granular Improved Embankment	All lanes	Lane A	10.29	123.2	25.4	33.9	21.60	24.2
		Lane B	9.30	123.0	25.5	34.7	20.95	27.8
		Lane C	9.78	123.8	24.77	33.3	20.74	21.2
	No Planned Difference		Yes	Yes	Yes	Yes	Yes	No
	All areas	Area 1,2	9.74	123.5	26.3	36.5	20.64	24.6
		Area 3	9.88	123.1	22.3	28.9	22.01	24.1
	No Planned Difference		Yes	Yes	No	No	Yes	Yes
TH-23 Crushed Aggregate Base	South & Middle Sections	Lanes A,B	9.37	129.8	14.4	100.4	42.05	16.75
		Lane C	10.62	129.8	10.8	50.7	21.33	8.31
	Lane C is weaker		No	No	Yes	Yes	Yes	Yes
	So. Area	Lanes A,B	9.79	129.9	15.0	110.7	46.45	19.38
	Middle Section	Lane C	10.38	129.8	9.8	28.0	18.55	7.95
	All other areas		9.54	129.8	12.8	75.0	33.14	12.31
	Lane C, middle section, is weaker		No	No	Yes	Yes	Yes	Yes
	Lanes A & B, south section, are stronger		No	No	Yes	Yes	Yes	Yes
US-280 Crushed Stone Base	All areas	Lane 4	11.57	148.2	35.1	117.4	34.31	18.53
		Lanes 1,2,3	11.95	147.4	47.9	198.6	50.29	46.46
	Lane 4 is weaker		No	No	Yes	Yes	Yes	Yes

NOTE: The shaded or black cells are those areas where the hypothesis was rejected based on a 95 percent confidence interval, and are inconsistent with the construction records and experimental plan.

- The LWD induces larger strains into the underlying materials. The measured deflections or responses are affected by a much larger area and depth than for the DSPA, GeoGauge, and DCP. The elastic modulus calculated from the deflections are dependent on the thickness and stiffness of the material being tested, as well as the stiffness of the supporting layers. In fact, some resulting elastic modulus values were lower than expected for the type of material being tested (TH-23 embankment). More importantly, the LWD found all of the hypotheses to be true were the layer thicknesses were well defined, but rejected many of the hypotheses for the materials where the layer thickness was less defined – the embankments.
- Both the GPR and EDG devices are dependent on the density and moisture content measurements made with other traditional test methods. Any errors within those traditional methods are included in the GPR and EDG results. More importantly, average moisture contents were assumed for each area in calculating the wet densities from the dielectric values measured with the GPR. Obviously, moisture contents are not constant within a specific area. Errors in the moisture content will be reflected in the wet density for a specific test. More importantly, varying plasticity of the fines and in the gradation of the material are difficult to identify with the GPR and EDG by themselves.

3.3 Laboratory Repeated Load Resilient Modulus Values

Laboratory repeated load resilient modulus tests were completed for all of the unbound materials at the average in place densities and moisture contents. The resilient modulus tests were performed in accordance with the provisional test procedure that resulted from NCHRP 1-28A. Twelve resilient modulus values were measured for each test specimen and are provided in the appendix. However, only one stress state was used for consistency in comparing the field estimated elastic modulus values from each NDT device to values measured in the laboratory. Table 26 summarizes the resilient modulus values measured in the laboratory at a low stress state. These laboratory measured resilient modulus values were assumed to be the target values.

As noted above, the test specimens were compacted to the average dry density and moisture content reported from the construction records and density testing during field tests with the different NDT technologies. The dry density, moisture content, and percent compaction that apply to each area tested are also summarized in table 26. Table 24 listed the optimum moisture contents and maximum dry densities resulting from M-D relationships for each material.

In general, the resilient modulus values measured in the laboratory increase with the quality of the material. The dense crushed stone base material placed along US-280 has the highest resilient modulus, while the low plasticity soil embankment prior to IC rolling has the lowest resilient modulus.

The high plasticity clay subgrade along SH-21, however, has a much higher resilient modulus than expected based on previous testing experience with this soil (Von Quintus,

1980 to 1996). One explanation for the larger values is that the moisture content at testing was well below the optimum moisture content. Moisture contents below the optimum value and approaching the plastic limit of the soil can significantly increase the resilient modulus. Similarly, the improved granular embankment placed along SH-130 was also found to have a larger value than expected. It is believed that the higher in place densities (above the maximum dry unit weight) account for the higher modulus values.

Table 26 – Summary of Repeated Load Resilient Modulus Values Measured in the Laboratory.

Project & Materials	Area		Dry Density, pcf	Moisture Content, %	Percent Maximum Density, %	Resilient Modulus, ksi
I-85 Low Plasticity Clay Embankment	Before IC Rolling	Section 1, Lanes B,C,D	103.0	21.6	0.91	2.5
	After IC Rolling	Section 1, Lanes B,C,D	108.0	16.9	0.96	4.0
TH-23 Embankment, Silt-Sand-Gravel Mix	South Section	Lanes A,B	121.0	8.2	0.98	16.0
	North Section	Lane B,C	122.4	9.1	1.00	16.4
SH-21 High Plasticity Clay	Area 1, with IC rolling	Lanes A,B	107.3	18.4	0.99	26.8
TH-23 Crushed Aggregate Base	Middle Area	Lane B	139.4	4.3	1.04	24.0
	South Area	All Lanes	141.1	4.2	1.03	24.6
SH-130 Improved Granular	Sections 2, 3	Lanes A,B	128.7	9.1	1.05	35.3
US-280 Crushed Stone	Areas 1,2,3		150.6	3.2	1.01	48.4
NOTES:						
<ul style="list-style-type: none"> Resilient modulus values are for a low confining pressure (2 or 3 psi) and repeated stress of 4 or 6 psi. This low stress condition is not based on any theoretical analysis. The one stress state was selected for consistency in comparing the field estimated elastic modulus values from each NDT device to values measured in the laboratory, which were considered the target values. Percent maximum density is based on the maximum dry unit weight or density from the moisture-density relationship (the maximum dry densities were included in table 24 for each material tested). 						

3.3.1 Comparison of Laboratory Measured and Field Estimated Modulus Values

The laboratory resilient modulus and field volumetric data were used to determine the laboratory resilient modulus for each area tested using the procedure and regression equations developed within the LTPP program. Regression equations were developed from the LTPP resilient modulus test data and physical properties of the test specimens to estimate the resilient modulus caused by small changes or deviations from the maximum dry density and optimum moisture content (Von Quintus and Yau, 2001). Table 27 summarizes the laboratory resilient modulus of each area tested. As shown, the GeoGauge and DSPA provided a reasonable ranking of each area tested, followed by the DCP. The deflection measuring devices did a poor job.



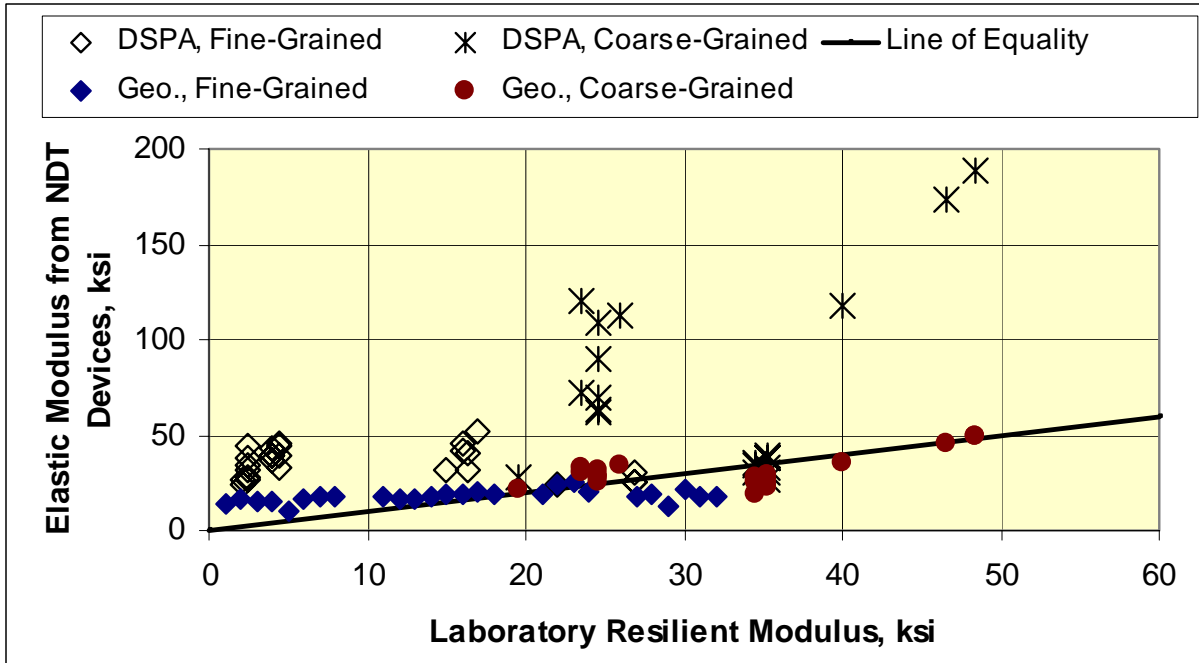
Figure 49 graphically compares the NDT test results and those values measured in the laboratory. As shown, the DCP and GeoGage provide a reasonable estimate of the laboratory values across all materials included in the Part A field study (less dense fine-grained soils to dense crushed stone bases). The elastic modulus values estimated from both the DSPA and LWD devices increase with increasing values measured in the laboratory, but have a significant bias. The DSPA over estimates the laboratory values, while the LWD under estimates those values and has the greater dispersion.

Table 27 – Elastic Modulus Values Estimated Directly from the NDT Technologies and Devices – No Field Adjustments, ksi.

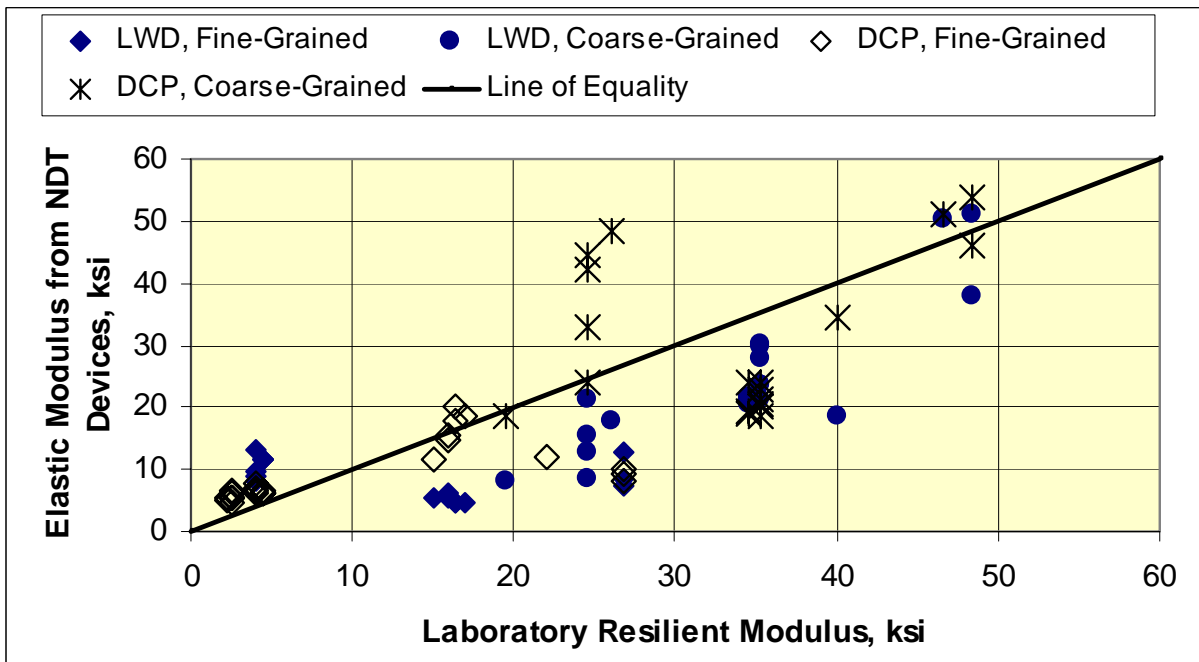
Project	Material	Area	Modulus, ksi				
			Lab.*	GeoGage	DSPA	DCP	LWD
I-85 Embankment Before IC Rolling	Low Plasticity Clay	Section 2, Lane A	2.2	10.6	24.1	5.0	---
		Section 1, All Lanes	2.5	15.4	30.0	5.9	---
		Section 2, Lanes B, C, D	2.5	17.0	36.6	5.2	---
I-85 Embankment After IC Rolling	Low Plasticity Clay	Section 1	4.0	16.8	30.4	6.9	9.99
		Section 2	4.5	19.0	40.4	6.2	11.78
TH-23 Embankment	Silt-Sand-Gravel Mix	So. Section, Lane C	15.0	13.2	31.1	11.5	5.6
		So. Sect., Lanes A,B	16.0	18.3	43.6	15.2	5.7
		No. Sect., Lanes B,C	16.4	17.8	35.7	19.0	4.7
		No. Sect., Lane A	17.0	22.0	51.7	18.5	4.7
SH-21 Subgrade	High Plastic Clay	No IC Rolling	22.0	19.6	23.6	11.9	---
		After IC Rolling	26.8	22.9	27.1	8.8	9.6
TH-23 Base	Crushed Aggregate Base	Middle Sect., Lane C	19.5	21.6	28.0	18.6	8.0
		North Section, All Lanes; Middle Section Lanes A, B	24.6	28.2	79.3	33.1	12.3
		South Section, Lanes A, B	26.0	33.0	110.7	46.4	19.4
SH-130 Improved Embankment	Granular	Section 3	34.5	19.4	33.3	20.7	24.1
		Sections 1, 2	35.3	26.4	34.3	21.3	24.6
US-280 Base	Crushed Stone	Area 4	40.0	35.1	117.4	34.3	18.5
		Areas 1, 2, 3	48.4	47.9	198.6	50.3	46.5

NOTES:

* - The repeated load resilient modulus values measured in the laboratory, but corrected to the actual dry density and moisture content measured for the specific section, in accordance with the LTPP procedure and regression equations.



(a) DSPA and the GeoGauge.



(b) Deflection-Based and DCP methods.

Figure 49 Comparison of laboratory resilient modulus and the elastic modulus values estimated with different NDT technologies and devices.

3.3.2 Adjustment of Field Results

It is expected that the calculated modulus values from the deflection based methods are affected by the underlying materials and soils. For example, the crushed stone base material placed in area 4 along US-280 near Opelika, Alabama is a stiff and dense material, even though it is weaker than the other areas tested. All other NDT devices estimated the modulus values to be about 35 ksi or higher, while the deflection based methods resulted in values less than 20 ksi. This in situ value is believed to be too low for this material. Conversely, the DSPA device significantly over-estimated the laboratory measured resilient modulus values. The crushed stone base was dry or significantly below the optimum moisture content during testing. It is believed that the surface of this dense-dry crushed stone is responding like a bound layer.

In addition, Von Quintus and Killingsworth found systematic differences between the elastic modulus calculated from FWD deflection basins and laboratory measured resilient modulus at the stress state under the FWD load. Laboratory measured resilient modulus to back-calculated elastic modulus ratios of 0.35 to 1.43 were reported and found to be dependent on the pavement structure, rather than soil type. Thus, there are differences between the field and laboratory conditions that can cause significant bias in the modulus values.

To compensate for differences between the laboratory and field conditions, an adjustment procedure was used to estimate the elastic modulus values from the different NDT technologies for making relative comparisons. This field adjustment is shown in the flow chart in Chapter 5 of this report, similar to the calibration procedure for nuclear density devices. The adjustment procedure assumes that the NDT response and modulus of laboratory prepared test specimens are directly related and proportional to changes in density and moisture content of the material. Figures 50 to 52 graphically compare the seismic modulus measured on the samples used in preparing an M-D relationship. As shown, the seismic modulus-moisture content relationship mimics the M-D curve.

To account for differences between the field and laboratory conditions, a ratio was calculated and used to adjust the elastic modulus measured with each NDT device. The ratio was determined from the average elastic modulus measured in an area without any anomalies and laboratory measured resilient modulus on test specimens compacted to the average dry density and moisture content measured during field testing. Table 28 lists the adjustment factors for the different materials and NDT devices.

Figure 53 compares the laboratory measured resilient modulus values to those estimated with different NDT devices but adjusted to laboratory conditions, while figure 54 presents the residuals (laboratory resilient modulus minus the NDT elastic modulus), assuming that the laboratory value is the target value. As shown, the adjusted elastic modulus from all devices compare reasonably well with the laboratory measured resilient modulus. The following tabulates the mean of the residuals and standard error for the NDT devices that provide a direct measure of material stiffness.

NDT Device	GeoGauge	DSPA	DCP	LWD
Mean Residual, ksi	-0.117	0.149	-0.078	0.614
Standard Error, ksi	2.419	4.486	3.768	5.884

In summary, the GeoGauge, DSPA, and DCP all provide good estimates with negligible bias of the laboratory measured resilient modulus values. The GeoGauge has the lower standard error. The LWD has a higher bias and over two times the standard error, in comparison to the GeoGauge.

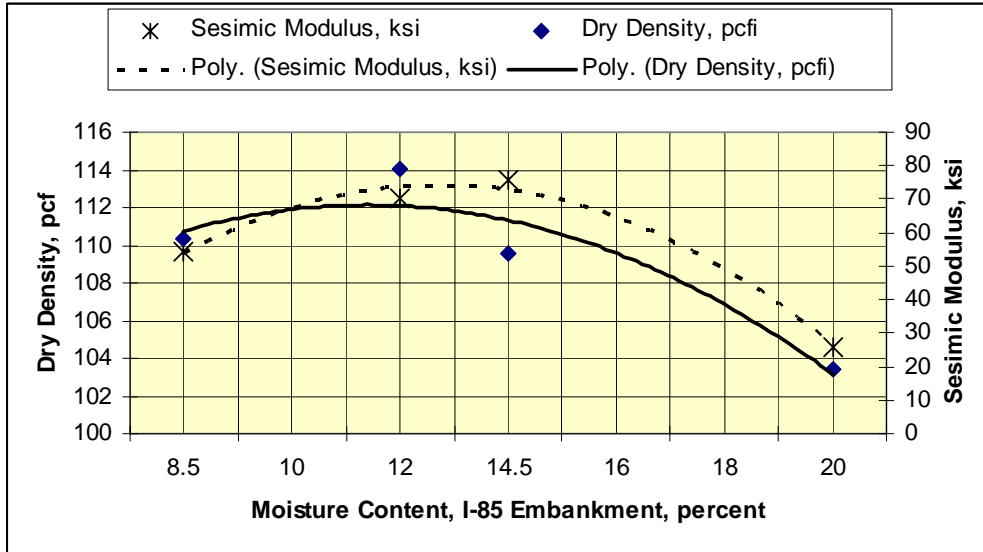


Figure 50 Graphical presentation of the seismic modulus measured on the samples used in preparing the M-D relationship for the I-85 low plasticity soil embankment.

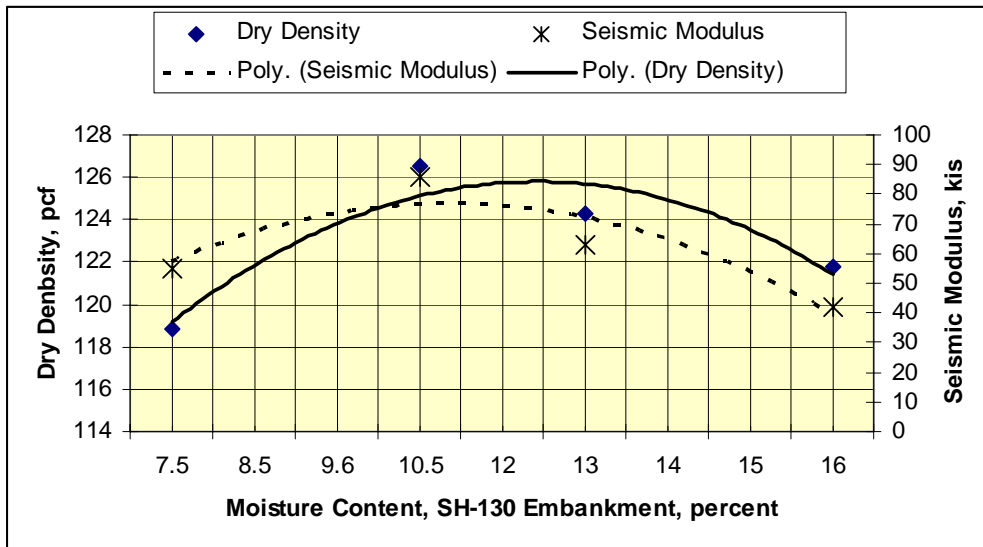


Figure 51 Graphical presentation of the seismic modulus measured on the samples used in preparing the M-D relationship for the SH-130 improved granular embankment.

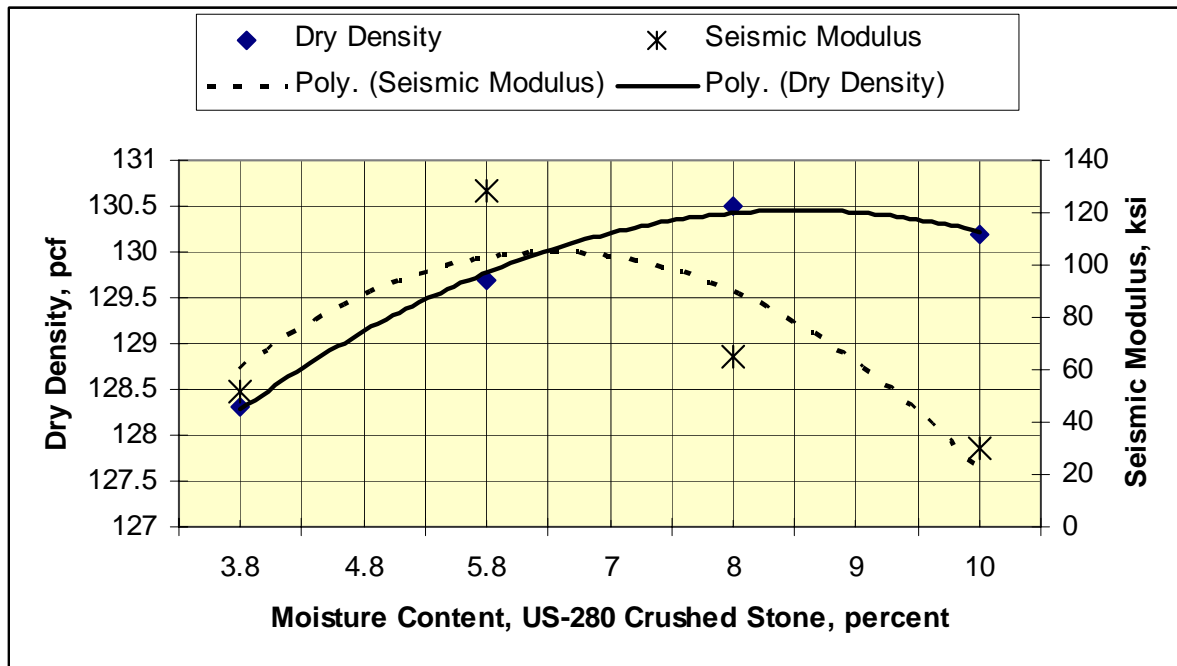
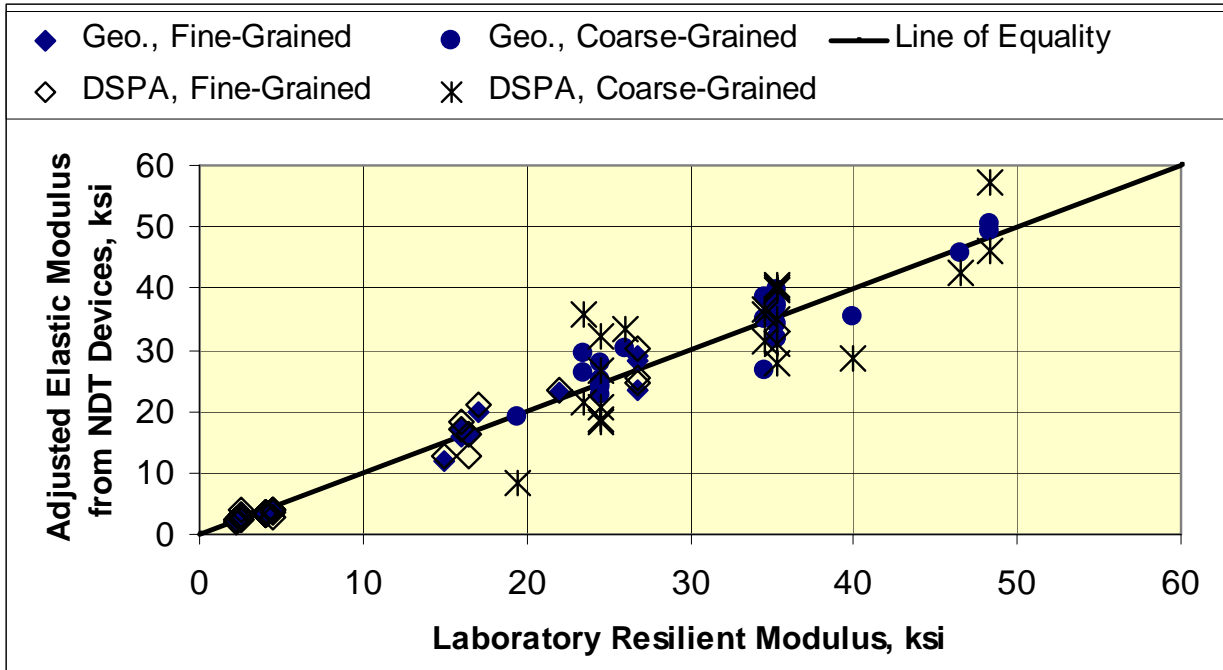


Figure 52 Graphical presentation of the seismic modulus measured on the samples used in preparing the M-D relationship for the US-280 crushed stone base.

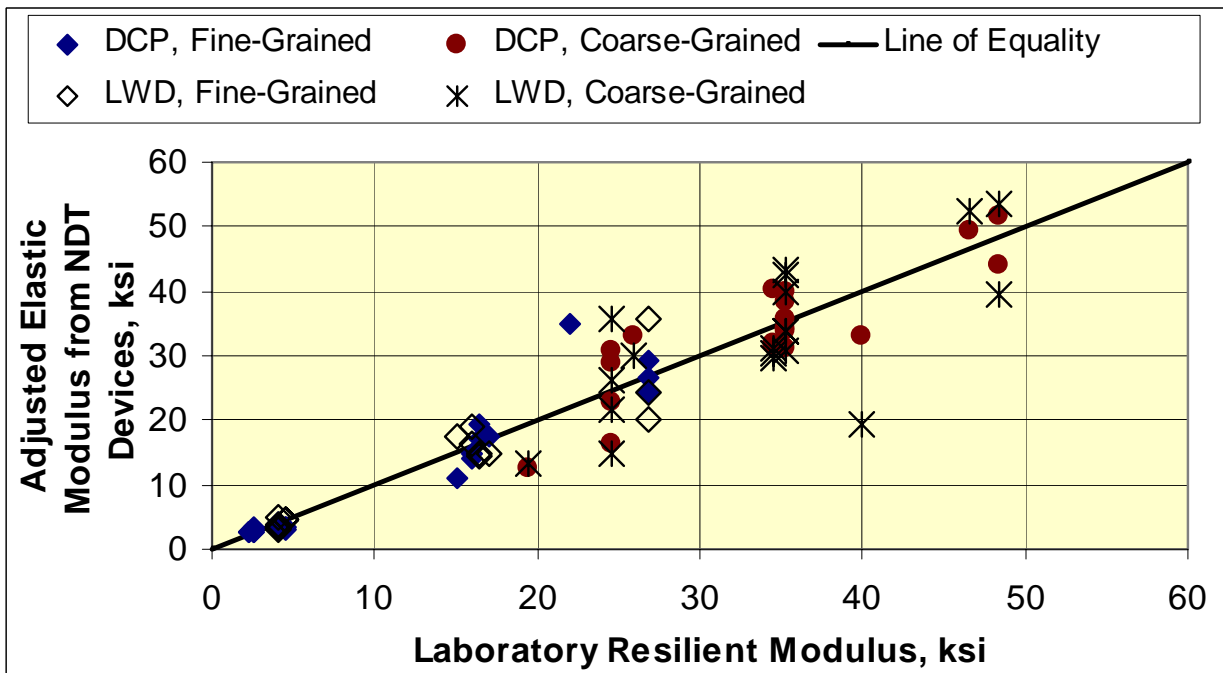
Table 28 – Adjustment Factors or Ratios Applied to the NDT Elastic Modulus Values to Represent Laboratory Conditions, ksi.

Project	Material	Percent Compaction	Percent of Optimum Moisture	Ratio or Adjust Factor			
				Geo.	DSPA	DCP	LWD
I-85 Embankment	Low Plasticity Clay	91	165	5.25	11.49	1.90	2.56
TH-23 Embankment	Silt-Sand-Gravel Mix	100	132	1.11	2.45	1.05	0.32
SH-21 Subgrade	High Plastic Clay	99	84	0.86	1.01	0.34	0.36
TH-23 Base	Crushed Aggregate	104	55	1.14	3.36	1.46	0.59
SH-130 Embankment	Improved Granular Mix	105	101	0.72	0.96	0.60	0.70
US-280 Base	Crushed Stone	101	52	0.99	4.09	1.04	0.96

The adjustment ratio or factor was determined by dividing the laboratory resilient modulus by the average elastic modulus measured by a specific NDT device from an area without anomalies.

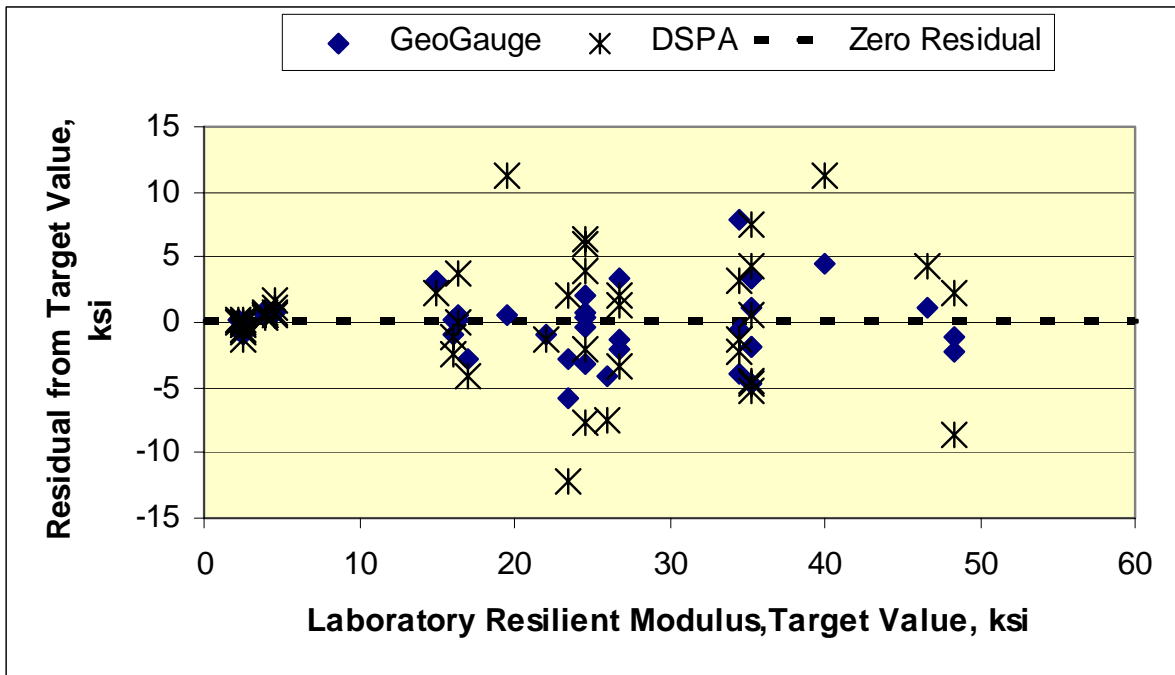


(a) DSPA and the GeoGauge.

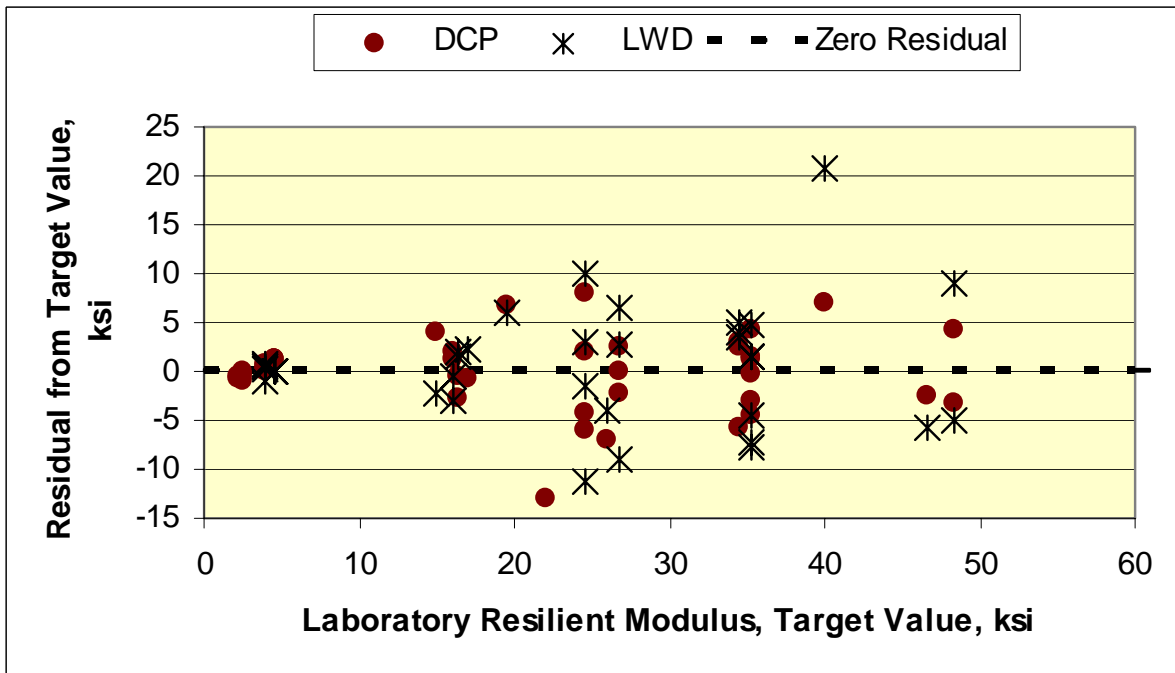


(b) Deflection-Based and DCP methods.

Figure 53 Comparison of laboratory resilient modulus and elastic modulus values estimated with different NDT technologies and devices, but adjusted to laboratory conditions.



(a) GeoGauge and DSPA.



(b) DCP and LWD.

Figure 54 Residuals (Lab Minus NDT Modulus) resulting from the adjusted NDT elastic modulus.

3.4 Comparison of Test Results Between Technologies

This section of Chapter 3 provides a brief comparison of the test results from different technologies.

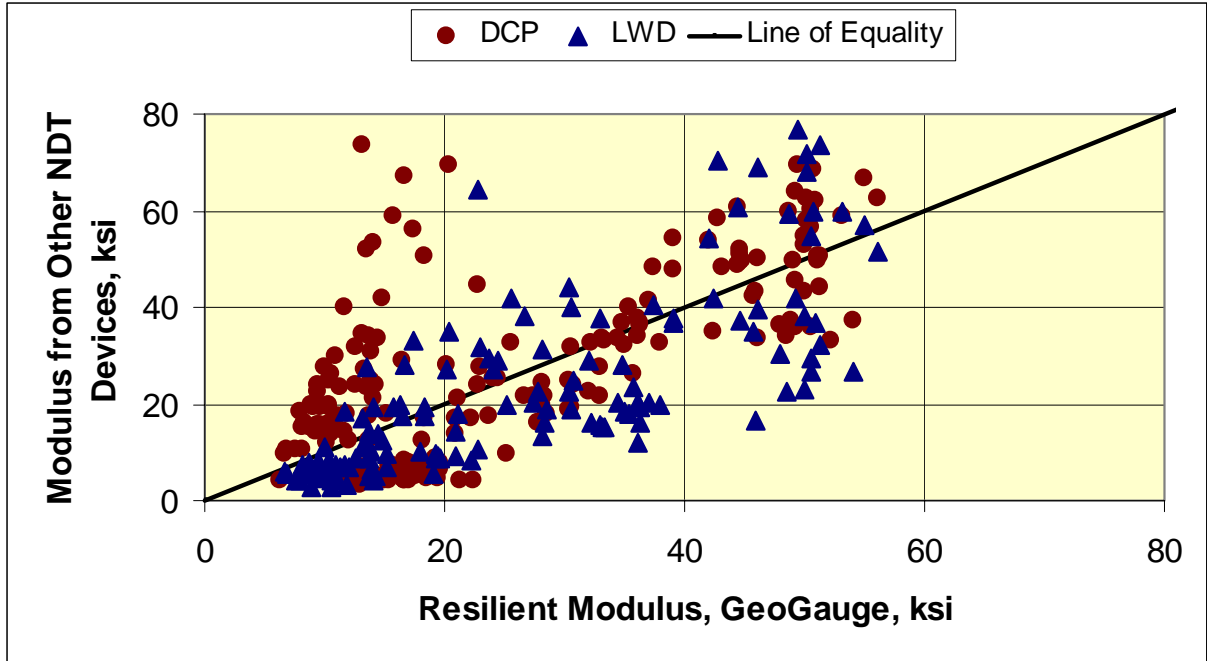
3.4.1 NDT Elastic Modulus Comparisons

Figure 55 compares the GeoGauge, DSPA, DCP, and LWD modulus values measured at the same test point, with and without the field adjustments that were presented in the previous section of this report. The following summarizes the comparisons between the NDT devices.

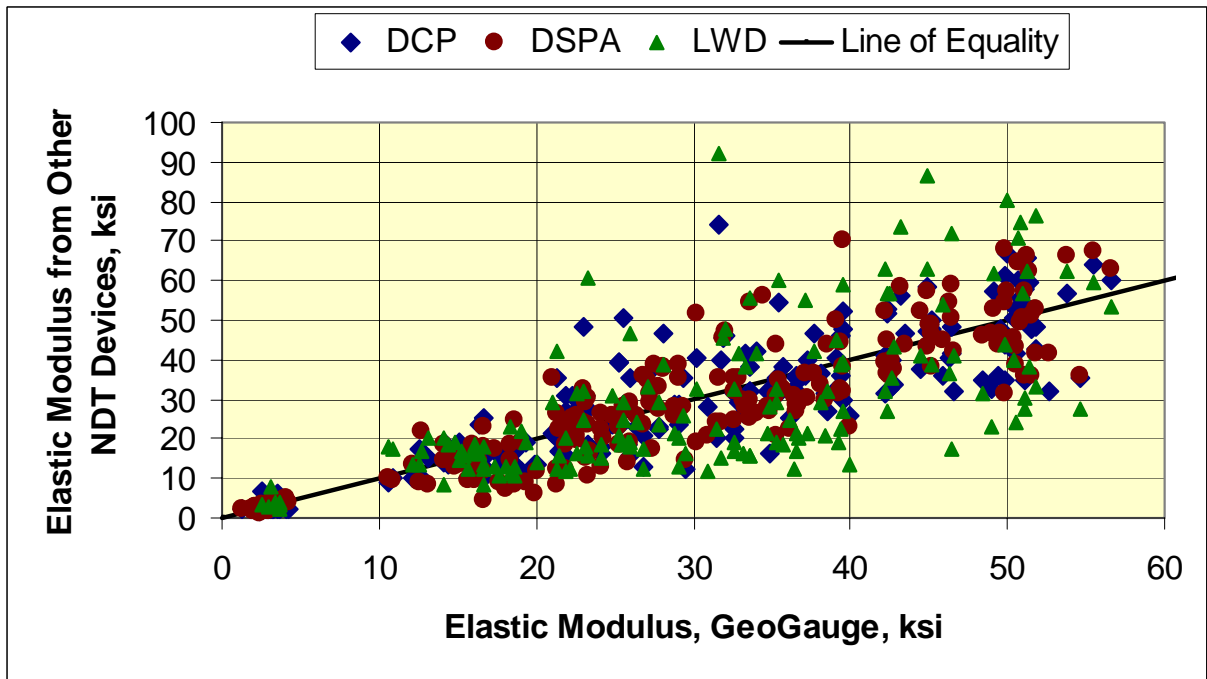
- Figure 55.a compares the unadjusted elastic modulus values. As noted previously, the modulus values from the deflection based methods are generally lower than for the other NDT technologies, while the DSPA results in larger values. One reason for these consistently lower values with the LWD is that the calculated modulus is being influenced by the underlying materials and soils, while the DSPA is measuring the response nearer the surface. The elastic modulus values from the DSPA are excluded from figure 55.a, because the unadjusted magnitudes are four times as large as the other NDT devices for some projects. This large difference would diminish the graphical comparison between the other devices (refer to figure 36).
- Figure 55.b presents a similar comparison of modulus values except that the field estimated values have been adjusted to laboratory conditions. The DSPA results are included in this graphical comparison. The adjustment procedure eliminated the bias between the different devices, but not the dispersion.

Figure 56 compares the average elastic modulus values measured within specific areas of a project. The dispersion of the average adjusted field values between the NDT devices is significantly less within a specific area. Thus, the average adjusted values to laboratory conditions from any of those devices can be used to estimate the resilient modulus of the material. The difference between the NDT devices is that more test points are required for those devices with greater variability. As such, an important comparison between the technologies is the coefficient of variation (COV) in measured modulus values within a common area.

Figures 57 to 60 compare the COV to the average elastic modulus measured by each device for the different areas tested, while figure 61 compares the COV between different technologies. As shown, the GeoGauge consistently has the lower COV and that value decreases with increasing material strength (figure 60). The reason for the higher COV values for the other devices is that the DCP penetration rate is dependent on the amount and size of coarse aggregate particles, while the LWD modulus values are dependent on the underlying materials. The DSPA is dependent on the moisture content variations nearer the surface, and the amount of fines in coarse-gained materials. The GeoGauge was found to be independent of type and size of aggregate and less dependent on the underlying materials.



(a) Comparison of elastic modulus values without field adjustments.



(b) Comparison of elastic modulus values with field adjustments.

Figure 55 Comparison of elastic modulus values determined from different NDT technologies at specific points for all projects.

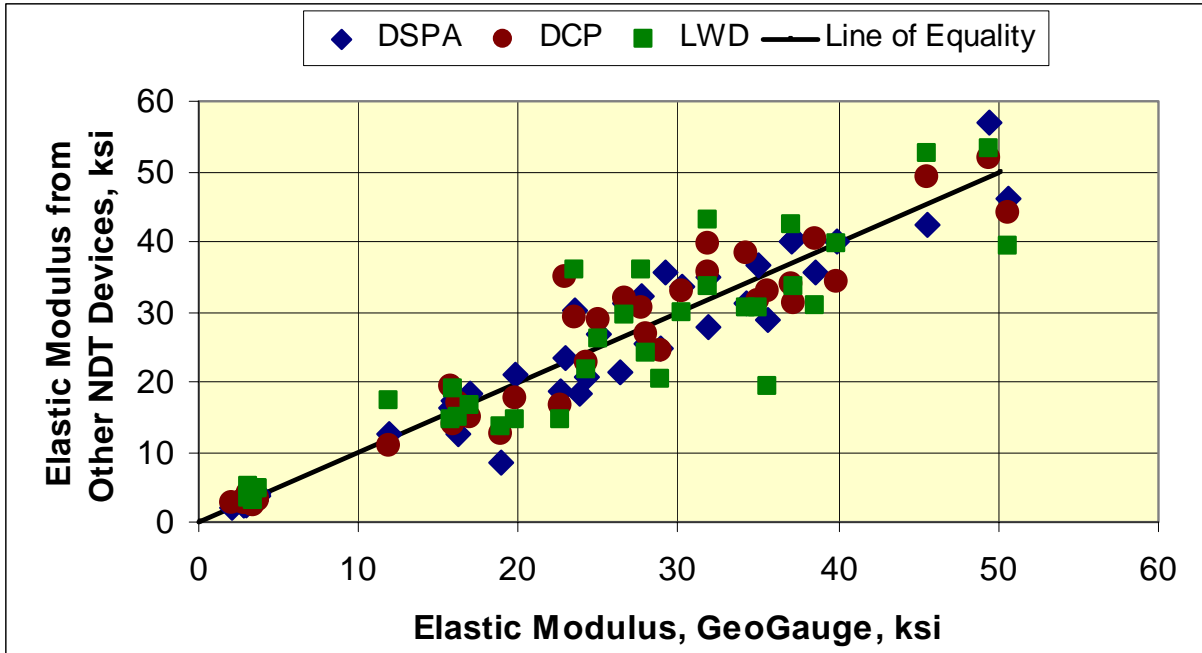


Figure 56 Comparison of average elastic modulus values determined from different NDT technologies for specific areas along each project.

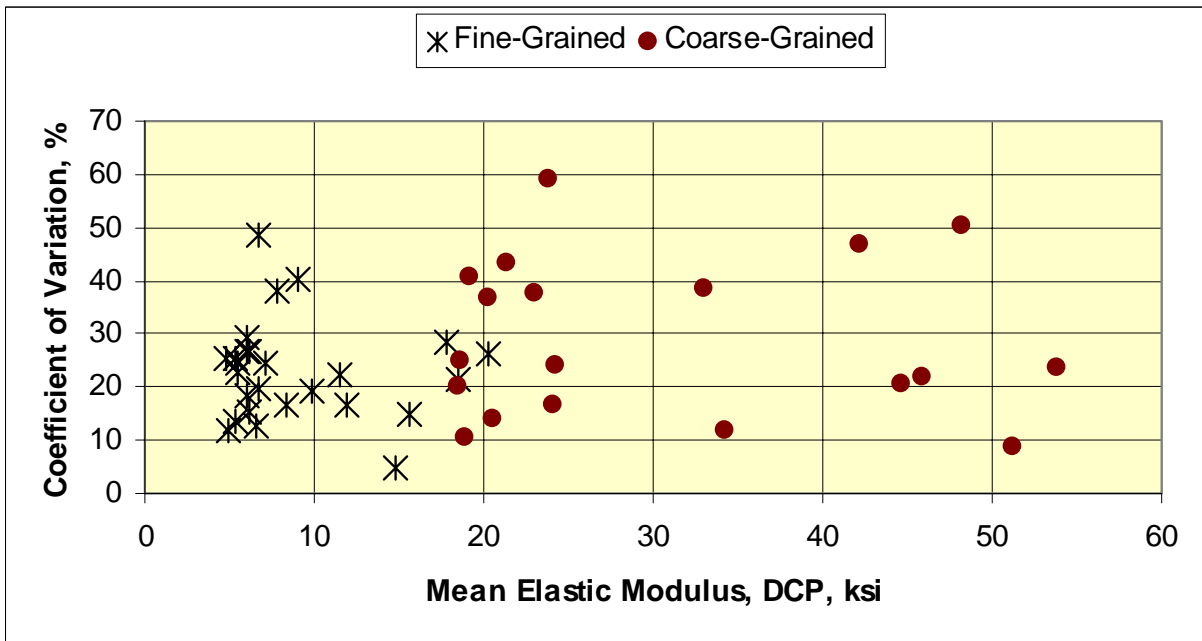


Figure 57 Relationship between the coefficient of variation and mean of the elastic modulus values calculated from the penetration rates of the DCP.

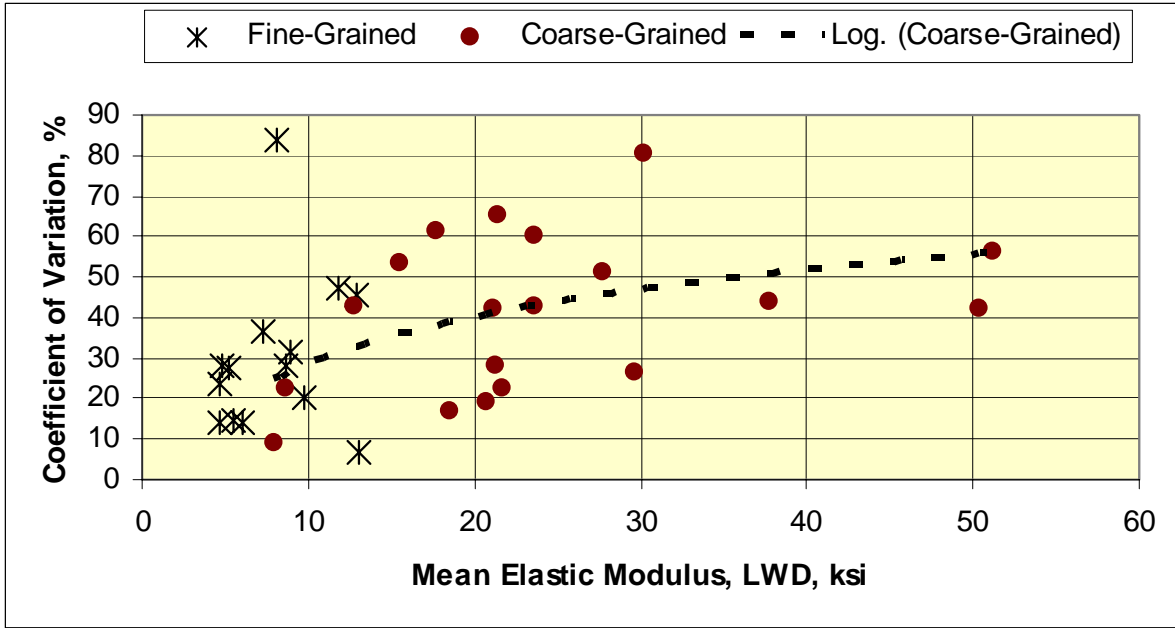
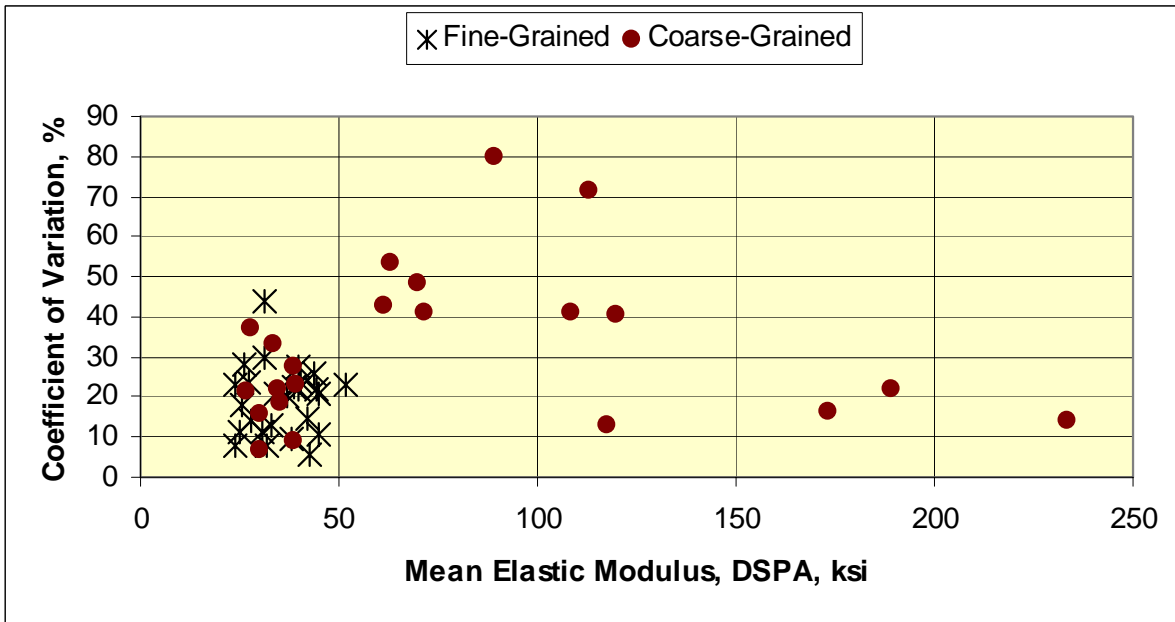


Figure 58 Relationship between the coefficient of variation and mean of the elastic modulus values calculated from deflections measured with the LWD.



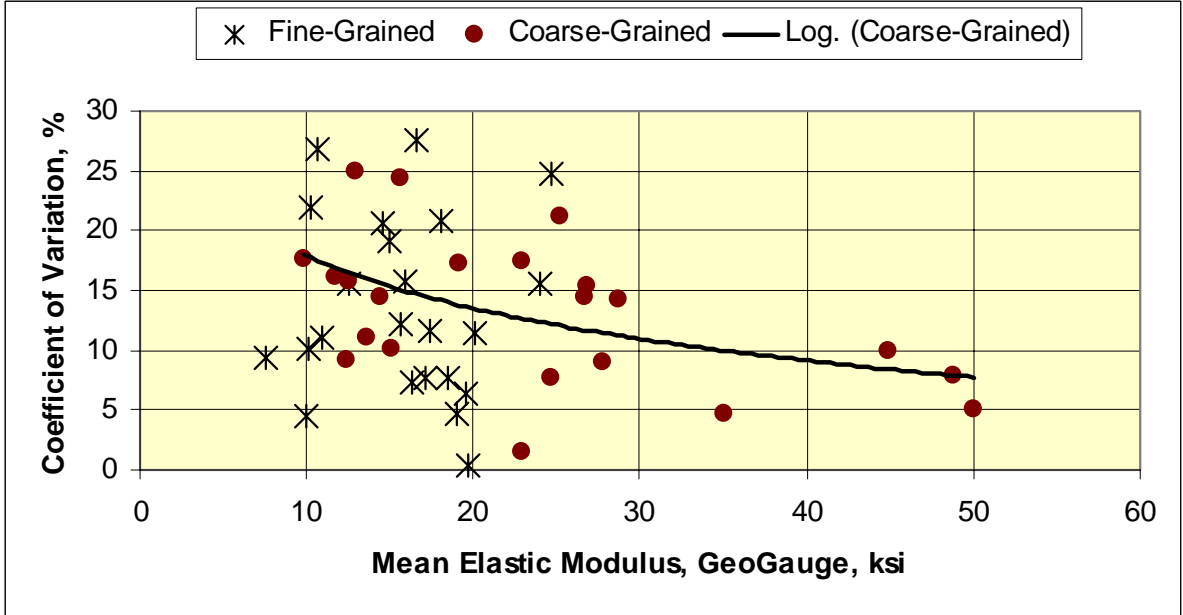


Figure 60 Relationship between the coefficient of variation and mean of the elastic modulus values determined from the GeoGauge responses.

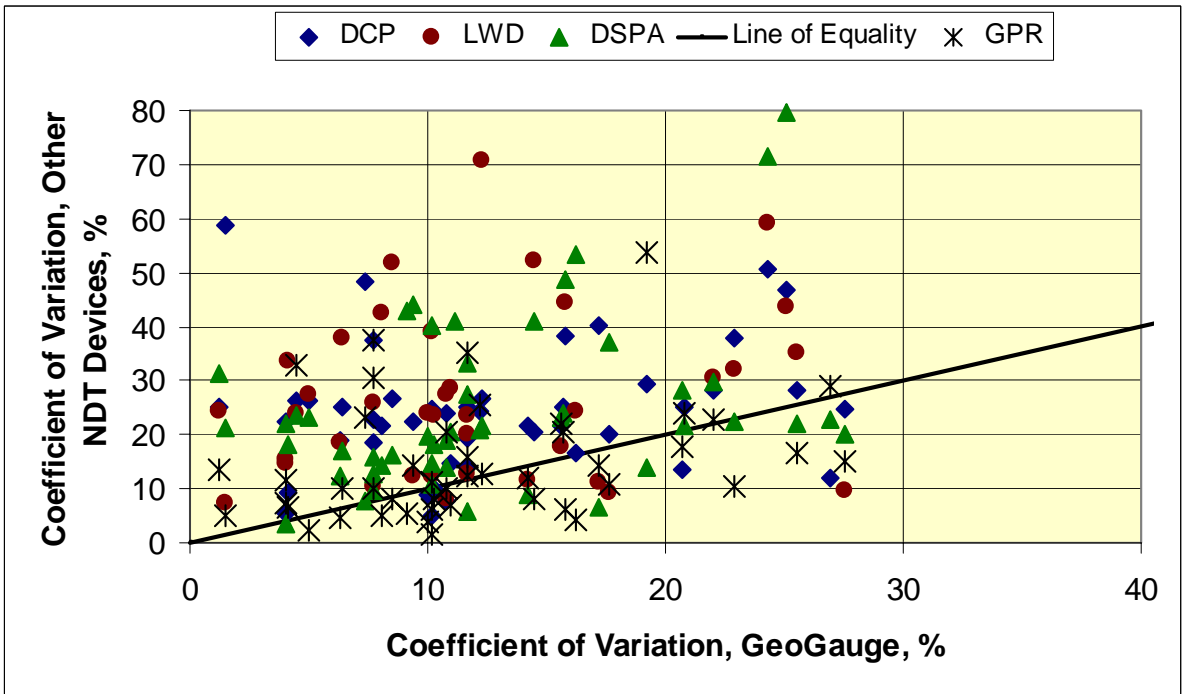


Figure 61 Comparison of the coefficient of variation in measured modulus and dielectric values between the different technologies.

As noted in section 3.1, the DCP and LWD found the unadjusted elastic modulus values for fine-grained materials to be consistently lower than for coarse-grained materials (refer to figures 27 and 32). The DCP and LWD can discriminate more closely to identify changes in these volumetric properties relative to gradation. This observation was not the case for the GeoGauge and DSPA (refer to figure 38).

The GeoGauge and DSPA apply small stress waves that make it difficult to detect differences in stiffness caused by changes in gradation and the amount of fines relative to the amount of moisture and level of dry density. This is another reason why the modulus values need to be adjusted back to a consistent laboratory condition for all devices in controlling and accepting construction of unbound layers.

3.4.2 NDT Volumetric Property Comparisons

The EDG and GPR were used to estimate the volumetric properties of the unbound materials. The following provides a summary of the response measurements to the dry densities obtained from construction records and traditional volumetric tests.

- Figure 62 compares the dielectric values to the dry densities measured with the EDG. As shown, no reasonable correlation was found between the different materials tested. In addition, no defined relationship was found between the two response measurements for the same material. This observation suggests that there are different parameters or features affecting the EDG and GPR results.
- Figure 63 compares the GPR dielectric values to the dry density measured with different devices – the EDG, nuclear density gauges, and sand-cone tests. As shown, no reasonable relationship was found; only a trend was identified between the GPR results and the densities obtained from construction records. As the dry density increased, the GPR dielectric values decreased.
- Figure 64 compares the dry densities measured with the EDG to those measured with a traditional nuclear density gauge. As shown, there are two definite groups of data – one for fine-grained soils and the other for crushed aggregate base materials. As the dry density increased between different materials, the density from the EDG also increased. Within each group, however, no reasonable relationship was found.

3.4.3 Volumetric – Modulus Comparisons

The in situ modulus and strength of the unbound materials are dependent on the density of the material being tested. The LTPP study conducted in 1997 found that the laboratory resilient modulus was dependent on dry density for all unbound materials (Von Quintus, et al., 1997). In fact, density and moisture content are two volumetric properties that have a significant affect on the modulus and strength of the material. Dry densities and moisture contents were recovered from the QA construction records for the different projects included in the study. This section of chapter 3 compares the densities and moisture contents measured with the NDT devices to the elastic modulus values measured with the other NDT devices, as well as with values measured during construction.

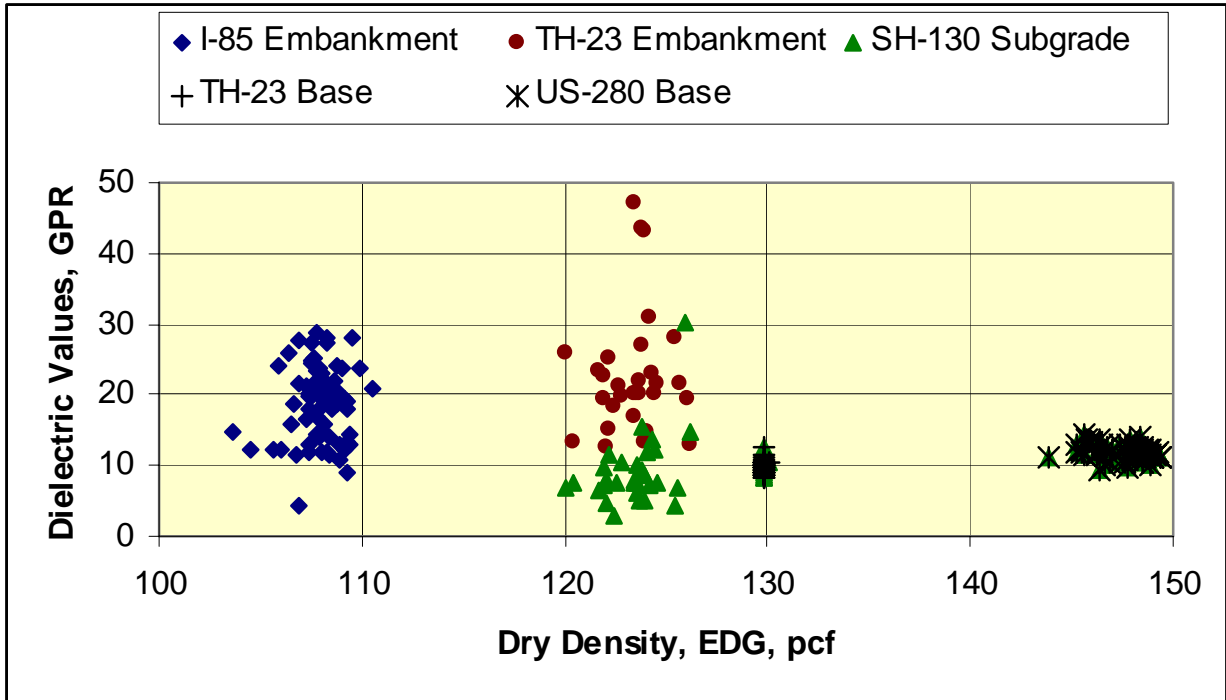


Figure 62 Comparison between the GPR dielectric values and the EDG dry densities measured along the different projects.

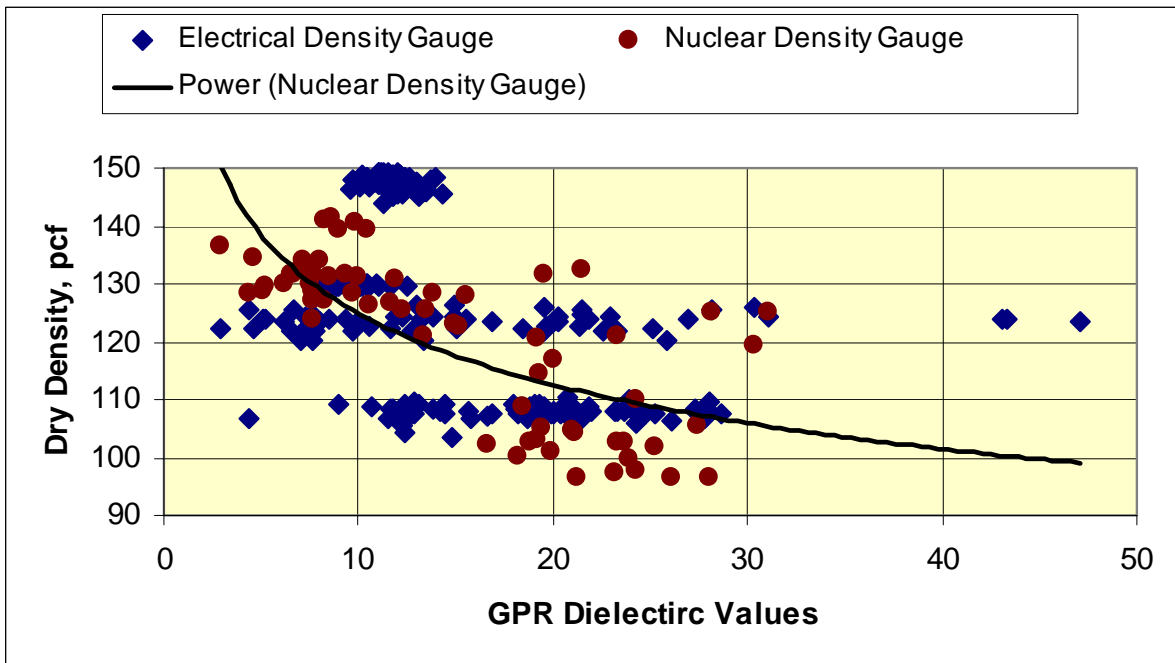


Figure 63 Relationship between the GPR dielectric values and dry density measured with nuclear and non-nuclear density gauges.

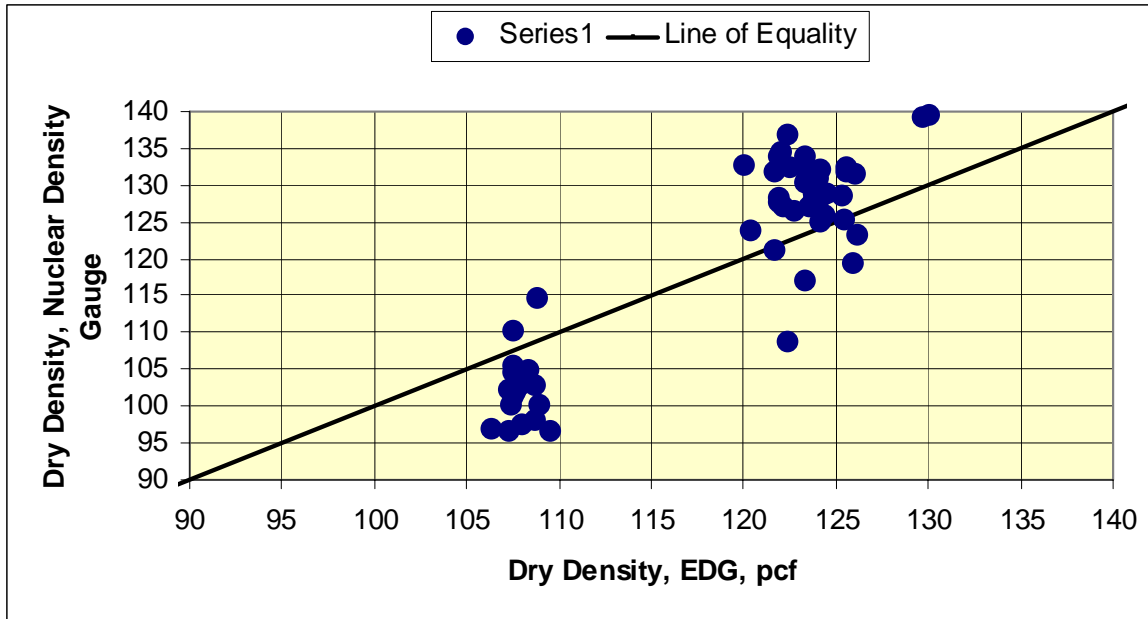
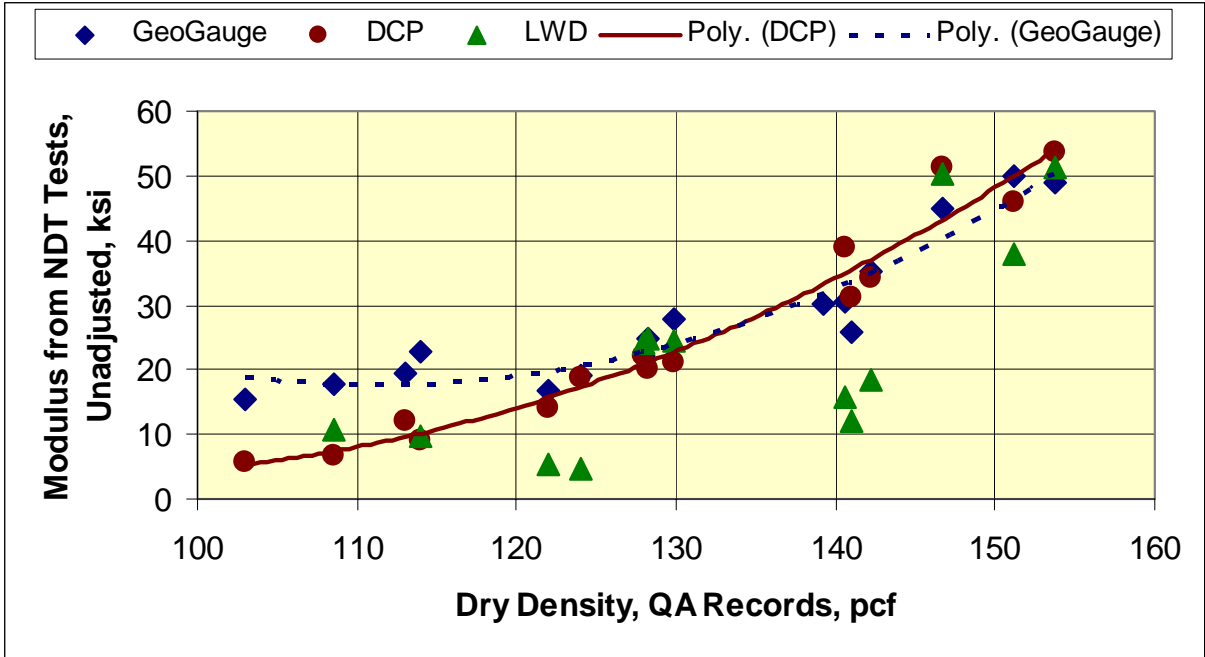


Figure 64 Comparison of the dry densities measured with the EDG and nuclear density gauge.

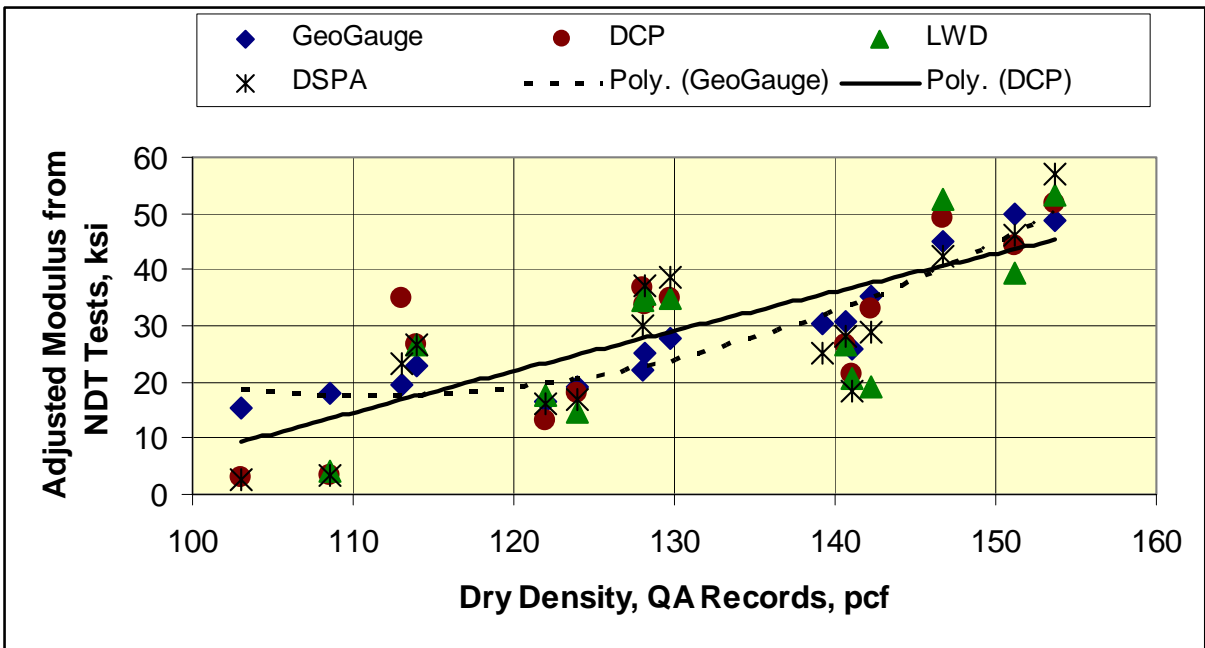
Figure 65 compares the average modulus values estimated from the different NDT technologies and the dry densities reported by the individual agencies during construction. The important observation from this comparison is that there is a good relationship between dry density and the DCP estimated elastic modulus, prior to adjusting the modulus values to laboratory conditions (figure 65.a). The resilient modulus from the GeoGauge is also related to the dry density of the material, but appears to become insensitive to dry density for less dense soils. The resilient modulus from the LWD is related to dry density, but has the greatest variation because of the influence of the underlying materials.

Figure 65.b graphically presents the same comparison included in figure 65.a, but using the adjusted modulus values. The GeoGauge and DSPA have similar relationships to dry density for both conditions. Conversely, the relationship for the DCP becomes less defined while it is improved for the LWD. Overall, the elastic modulus values resulting from each NDT device are related to the dry density across a wide range material. The GeoGauge has the better relationship to dry density, followed by the DSPA and DCP. Thus, the GeoGauge was the primary device used in comparing the elastic modulus to the EDG and GPR results.

The dry density and moisture contents from the QA records were fairly disperse and were not taken at each NDT test location or individual area. As such, the QA data can only be used to evaluate the results for different types of materials, rather than actual density variations within a project. In other words, figure 65 showed the effect of dry density on resilient modulus over a wide range of materials. The EDG, however, was used to measure the density and moisture contents at specific test locations for the other NDT devices.



(a) Unadjusted modulus values.



(b) Modulus values adjusted to laboratory conditions.

Figure 65 Effect of dry density for different unbound materials on the modulus values as measured by different NDT technologies.

Figure 66 compares the dry densities measured with the EDG and modulus values estimated from the GeoGauge and DCP. The resilient modulus increases with increasing dry density, which is consistent with previous experience. However, there are clusters of data for the EDG that correspond to the different unbound materials tested. Within each data cluster, the correspondence between dry density and resilient modulus is poor for both devices.

This observation suggests that there are other factors that impact the resilient modulus within a specific area; for example, the water content and amount of coarse aggregate varying within each data cluster. The EDG did not measure large variations in moisture content within each area. In summary, the within project area variation of the modulus values appear to be more dependent on other properties than dry density (i.e.; moisture content, gradation, etc.).

Figure 67 compares the resilient modulus measured with the GeoGauge and the dielectric values measured by GPR. No clear correspondence was found between the dielectric values and resilient modulus values. Specifically, a wide range of dielectric values and elastic moduli were measured, but no consistent relationship was found between the two properties. Thus, parameters or properties of the material that affect elastic modulus within an area have little to no effect on the dielectric values.

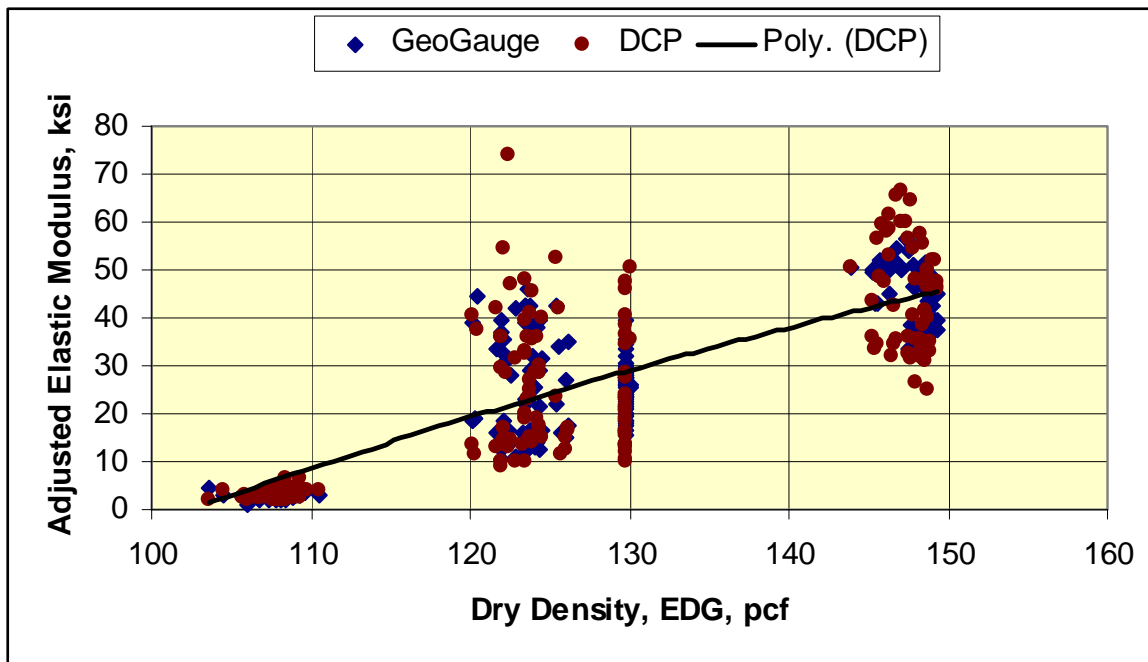


Figure 66 Comparison of the elastic modulus and dry density measured by the EDG.

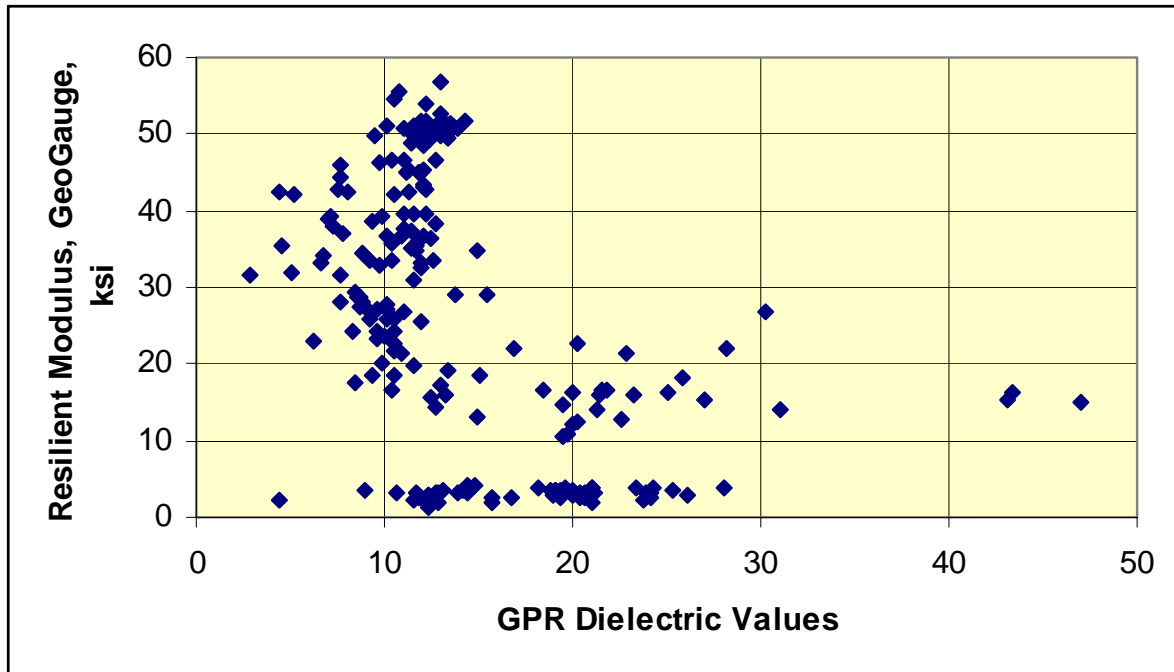


Figure 67 Comparison of the GPR dielectric value to the resilient modulus measured with the GeoGauge.

3.5 Summary of Nondestructive Testing of Unbound Materials

This section provides a summary of the testing of unbound materials from the Part A field study to confirm that the NDT devices can detect changes in the physical condition of the material.

- Identification of Material Anomalies and Features – The DSPA and GeoGauge devices had the highest success rates for identifying an area with anomalies with rates of 86 and 79 percent, respectively (table 25). The DCP and LWD identified about two-thirds of the anomalies, while the GPR and EDG had unacceptable rates below 50 percent.
- Repeatability measurements were conducted with each NDT device, with the exception of the DCP.
 - The LWD had low standard deviations (less than 0.5 ksi) that were less dependent on material stiffness. However, the elastic modulus for many of the layers was less than expected and measured by the other devices. It is expected that the supporting layers had an effect on the results by lowering the elastic modulus.
 - The GeoGauge had a standard deviation for repeatability measurements varying from 0.3 to 3.5 ksi and are material dependent.
 - The DSPA had the lowest repeatability with a standard deviation varying from 1.5 to 21.5 ksi. The reason for this higher variation in repeat readings is that the DSPA sensor bar was rotated relative to the direction of the roller, while the other devices were kept stationary or do not have the capability to detect anisotropic conditions.

No significant difference, however, was found relative to the direction of testing.

Figure 68 compares the seismic modulus measured parallel to roller direction to the difference between the modulus parallel and perpendicular to roller direction.

- The EDG is very repeatable with a standard deviation in density measurements less than 1 pcf, while the GPR had poor repeatability – based on point measurements.

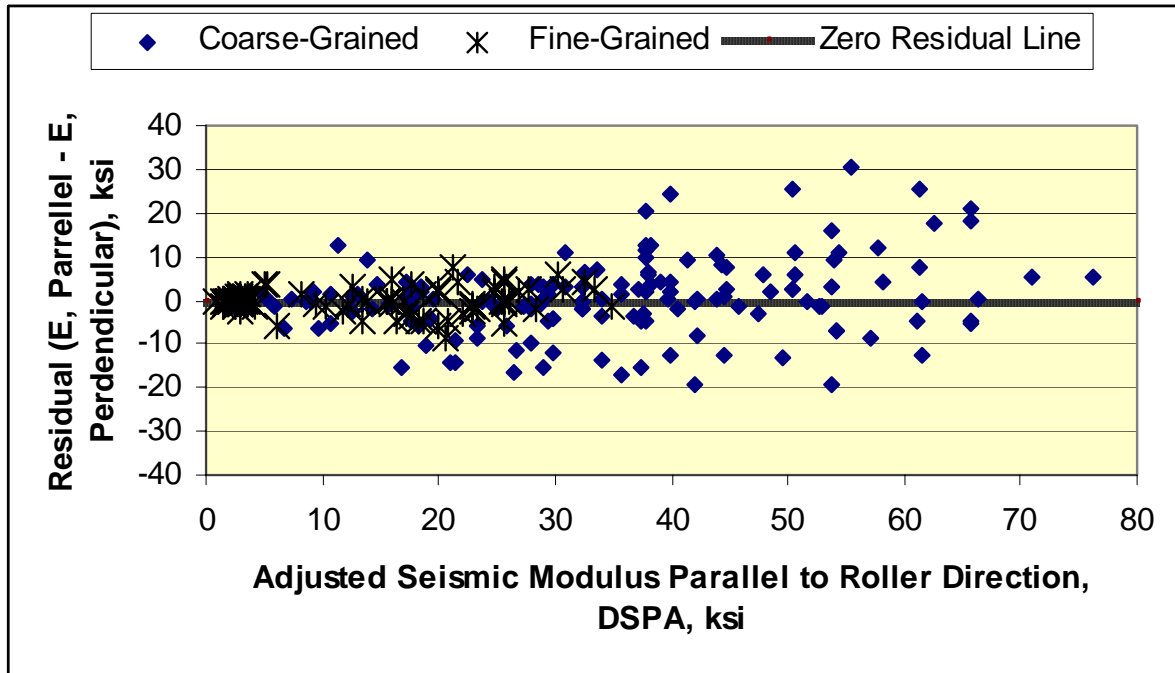


Figure 68 Comparison of the DSPA seismic modulus values measured parallel to roller direction to the difference between the modulus values parallel and perpendicular to roller direction.

- The coefficient of variation (COV) was used to compare the construction variability estimated with the different NDT devices. The EDG had the lowest COV with values less than 1 percent. The GeoGauge had an acceptable value of 15 percent, followed by the DSPA, LWD, DCP, and GPR.
- The GPR and EDG are dependent on the accuracy of other tests in estimating volumetric properties (density and moisture contents). Any error in the calibration of these devices for the specific project and material are directly reflected in the resulting values. This is one reason why the GPR and EDG devices did a poor job in identifying the areas with anomalies.
- Repeated load resilient modulus tests were performed in the laboratory for characterizing and determining the target resilient modulus for each material and layer included in the Part A field study. All NDT devices that estimate resilient modulus resulted in low residuals (laboratory resilient modulus minus the NDT elastic modulus). However, the

GeoGauge and DCP resulted in the lowest standard error. The LWD resulted in the highest residual and standard errors (figures 53 and 54).

- The modulus resulting from all devices can be easily related to the value measured in the laboratory – resilient modulus (figure 53). When adjusted to laboratory conditions, the average elastic modulus resulting from all NDT devices that estimate resilient modulus are related (figures 55 and 56). In addition, the average modulus resulting from these devices is related to the average dry density of the material being tested (figure 65), which is consistent with previous experience from the LTPP program.
- The DSPA and DCP result in modulus values that represent specific materials being tested. The measured responses from both devices can be used to estimate the modulus of a surface material without significant modification. The GeoGauge results are minimally affected by the supporting materials, while the LWD can be significantly affected by the supporting materials and thickness of the material being tested. Thickness deviations and variable supporting layers are reasons why the LWD had a low success rate in identifying areas with anomalies. Conversely, the DCP can be significantly affected by the varying amounts of aggregate particles in fine-grained soils.
- The DCP and LWD discriminated between fine and coarse-grained materials, while the GeoGauge and DSPA did not.
- Poor correlations were found between the NDT devices that estimate resilient modulus and those devices that estimate volumetric properties.
- The IC rollers used on different projects did not produce comparable results to the NDT devices. However, these rollers are believed to be worth future investments in monitoring the compaction and densification of unbound materials. One potential disadvantage with these rollers is that they may bridge localized weak areas.
- The GPR device resulted in close estimates to the layer thickness placed. None of the other NDT devices have the capability or same accuracy to determine the thickness of the unbound layer.